

Beryllium isotopic composition and Galactic cosmic ray propagation

Paolo Lipari^{1,*}

¹*INFN sezione Roma “Sapienza”*

The isotopic composition of beryllium nuclei and its energy dependence encode information of fundamental importance about the propagation of cosmic rays in the Galaxy. The effects of decay on the spectrum of the unstable beryllium-10 isotope can be described introducing the average survival probability $P_{\text{surv}}(E_0)$ that can be inferred from measurements of the isotopic ratio Be10/Be9 if one has sufficiently good knowledge of the nuclear fragmentation cross sections that determine the isotopic composition of beryllium nuclei at injection. The average survival probability can then be interpreted in terms of propagation parameters, such as the cosmic ray average age, adopting a theoretical framework for Galactic propagation. Recently the AMS02 Collaboration has presented preliminary measurements of the beryllium isotopic composition that extend the observations to a broad energy range ($E_0 \simeq 0.7\text{--}12$ GeV/n) with small errors. In this work we discuss the average survival probability that can be inferred from the preliminary AMS02 data, adopting publically available models of the nuclear fragmentation cross sections, and interpret the results in the framework of a simple diffusion model. This study shows that the effects of decay decrease more slowly than the predictions, resulting in an average cosmic ray age that increases with energy. An alternative possibility is that the cosmic ray age distribution is broader than in the models that are now commonly accepted, suggesting that the Galactic confinement volume has a non trivial structure and is formed by an inner halo contained in an extended one.

I. INTRODUCTION

It is now well established that most of the cosmic rays (CR) observed at the Earth in a broad energy range that extends from $E \sim 10^9$ eV to at least $E \sim 10^{16}$ eV are of Galactic origin, and are generated in the Milky Way, where they remain partially confined by interstellar magnetic fields for a time of order 1–100 Myr. Understanding the properties of CR propagation, and determining the duration and energy (or rigidity) dependence of their Galactic residence time remains a problem of crucial importance for high energy astrophysics.

The study of the flux of the unstable nucleus beryllium-10 (Be10) has been recognised for a long time as a crucially important source of information about the properties of CR propagation. This is because the Be10 decay time ($T_{1/2} \simeq 1.387 \pm 0.012$ Myr) is comparable with the average CR Galactic residence time, and therefore decay can be a significant, or dominant “sink” mechanism in the formation of the spectrum. Comparing the spectral shape of Be10 with those of the stable isotopes Be9 and Be7, allows in principle to measure the effects of decay, and then infer properties of Galactic propagation.

The experimental study of the spectra of individual isotopes, is however a very difficult task, and until now measurements for beryllium have been obtained only at low energy (kinetic energy per nucleon $E_0 \lesssim 2$ GeV) and with rather large errors. Recently, at the 37th International Cosmic Ray Conference in Berlin, the AMS02 Collaboration has presented preliminary measurements of the beryllium isotopes spectra and of the Be10/Be9 ratio with small errors (of order 10–20%). and in a broad energy range ($E_0 \simeq 0.7\text{--}12$ GeV). These results can be of great value to find answers to some important open questions about CR Galactic propagation.

In this work, waiting for the publication of the AMS02 observations on the isotopically separated beryllium spectra, we discuss the preliminary results presented at the ICRC, and the best methods to study their astrophysical implications.

*Electronic address: paolo.lipari@roma1.infn.it

We argue here that it is both convenient and appropriate to divide this study into two steps. In the first step, one starts from measurements of the isotopic ratio Be10/Be9, to estimate the average survival probability $P_{\text{surv}}(E_0)$, a quantity that describes the effects of decay on the Be10 spectrum. The main uncertainty in this first step is associated to the description of the nuclear fragmentation cross sections that determine the beryllium isotopic ratio at production. In the second step one interprets the results on P_{surv} to estimate CR propagation parameters. This second step is model dependent and is possible only assuming a theoretical framework that must be carefully discussed.

This paper is organised as follows: in the next section we define the average survival probability $P_{\text{surv}}(E_0)$ that encodes the effects of decay of the spectrum of the unstable beryllium-10 isotope, and discuss how it is possible to infer P_{surv} from measurements of the isotopic Be10/Be9.

In section III we discuss the (energy dependent) cosmic ray age distribution and how it determines the average survival probability.

The following section discusses in detail the 1-Dimensional ‘‘Minimal Diffusion Model’’ where propagation (for particles at a fixed energy) is described by two parameters: a diffusion time T_{diff} for escape from a homogeneous Galactic confinement volume, and the vertical size Z_{halo} of this volume. This model captures the main features of the models that are in common use to interpret cosmic ray measurements, but is also sufficiently simple that it is possible to calculate the average survival probability (and several other interesting quantities) obtaining exact analytic expressions. This can be both convenient and instructive, to develop an understanding of the problem.

In section V we use these results to compute allowed intervals for the diffusion time and the halo size that can be inferred from the AMS02 preliminary data. The main source of systematic error in this exercise is the estimate of the nuclear fragmentation cross sections that are used to obtain the average survival probability from the measurements of the isotopic ratio.

The final section discusses critically the results, and their possible implications. The most intriguing result that emerges from the preliminary AMS02 measurements is that the isotopic ratio Be9/Be10 grows with energy more slowly than expectations based on current diffusion based models. If these results are confirmed, this discrepancy can perhaps be explained as the effect of an incorrect description of the nuclear fragmentation cross sections. The alternative possibility is that the diffusion models commonly used to interpret the CR observations are not adequate and must be revised.

II. FROM THE ISOTOPIC RATIO TO THE AVERAGE SURVIVAL PROBABILITY

In this paper we argue that it is natural and convenient to study the effects of decay on the Be10 spectrum, introducing (following [1]) the average survival probability $P_{\text{surv}}(E_0)$ (with E_0 the kinetic energy per nucleon). This quantity is defined as:

$$P_{\text{surv}}(E_0) = \frac{\phi_{10}(E_0)}{\phi_{10}^{(0)}(E_0)} \quad (1)$$

where the numerator is the Be10 flux at the boundary of the heliosphere after correcting for solar modulation effects, and the denominator is the same flux *calculated* under the hypothesis that the nuclei are stable.

This definition might appear problematic, because the denominator in Eq. (1) is not a directly measurable quantity, however this difficulty can be circumvented, estimating the ‘‘no-decay’’ Be10 flux, using the observed flux of the stable isotope beryllium-9 and applying appropriate corrections, as discussed below, after briefly presenting the observations of the beryllium isotopic ratio Be10/Be9 in the energy range $E_0 \gtrsim 1$ GeV.

A. Measurements of the Be10/Be9 ratio for $E_0 \gtrsim 1$ GeV

The AMS02 preliminary data [2] on the beryllium isotopic ratio Be10/Be9 are shown in Fig. 1, together with the data of the ISOMAX balloon experiment [3], that has also published a measurement of this ratio above $E_0 \simeq 1$ GeV.

The AMS02 measurement of the isotopic ratio grows slowly from $R \simeq 0.15$ at the lowest energy to $R \simeq 0.32 \pm 0.03$ at $E_0 \simeq 8$ GeV, then the ratio for the next two points is smaller, and at the highest energy ($E_0 \simeq 11$ GeV) the ratio takes the value $R \simeq 0.22 \pm 0.04$. These results can be well described with a simple logarithmic dependence:

$$R_{\text{AMS}}(E_0) \simeq (0.16 \pm 0.02) + (0.11 \pm 0.03) \log_{10} \left(\frac{E_0}{\text{GeV}} \right) . \quad (2)$$

Combining quadratically statistical and systematic errors, this (purely phenomenological) fit corresponds to an acceptable $\chi_{\text{min}}^2 \simeq 8.2$ for 11 d.o.f. It is however tempting to speculate that the isotopic ratio grows more slowly for E_0 close to 10 GeV. In fact eliminating the three highest energy points, the best fit has $\chi_{\text{min}}^2 = 1.9$, with a reduction of 6.3 units. The existence of such an effect has only a weak statistical significance, but if real, would have important implications.

The ISOMAX data points have large errors, and correspond to broad energy bins and therefore provide a weaker constraint on the isotopic ratio. Using again a simple logarithmic form for the energy dependence of the ratio the data can be (roughly) represented as:

$$R_{\text{ISO}}(E_0) \simeq (0.25 \pm 0.06) + (0.20 \pm 0.12) \log_{10} \left(\frac{E_0}{\text{GeV}} \right) , \quad (3)$$

with a best fit that is a little larger than for AMS02 and grows more rapidly with energy.

It should be noted that a measurement of the beryllium isotopic composition above 1 GeV has also been obtained by the superconducting magnet instrument for light isotopes (SMILI) [4]. This experiment has found that out of 26 observed beryllium events, seven are of Be10, and this, according to the authors, corresponds to a survival probability consistent with unity, and has been interpreted as an upper limit on the ‘‘mean lifetime of cosmic rays’’ of 6 Myr at 97.5% confidence level. We will not discuss further the SMILI results, that should however be kept in mind.

Other measurements of the beryllium composition have been obtained at lower energy [5, 6].

B. Solar modulation effects

The measurements of the isotopic ratio are performed in the vicinity of the Earth, where the CR spectra are distorted by time dependent solar modulation effects. It is convenient to correct for these, reasonably well understood effects, and obtain the isotopic ratio in the local interstellar medium. To calculate this correction we have used the so called force field approximation (FFA) that describes the solar modulations effects assuming that (positively charged) CR particles during propagation from the boundary of the heliosphere to the Earth lose an amount of energy proportional to their electric charge: $\Delta E \simeq e Z V(t)$, where $V(t)$ is a time dependent potential associated to the heliospheric electromagnetic fields. The spectra at the Earth and in the local interstellar medium are then related by the equation:

$$\phi_{\oplus}(E) = \frac{p^2}{p_0^2} \phi_{\text{LIS}}(E + \Delta E) \quad (4)$$

where p and p_0 are the momenta that correspond to the energies E and $E + \Delta E$.

Information on the CR spectra at the boundary of the heliosphere have been obtained by the Voyager satellite, and comparing with the spectra measured by AMS02, one finds that Eq. (4) can provide a reasonably accurate description of the (time averaged) beryllium spectra using a potential $V \simeq 0.50$ GV, a value that is also consistent with the spectral distortions suffered by protons and other nuclei.

In the FFA model, the total energy loss of a nucleus due to solar modulations depends only on its electric charge Z , but this implies that the energy loss per nucleon of different isotopes are not identical. It is however straightforward to take this effect into account. Using Eq. (4), the beryllium isotopic ratio in the local interstellar medium can be written in terms of the observed spectra as:

$$\frac{\phi_{10}^{(\text{LIS})}(E_0)}{\phi_9^{(\text{LIS})}(E_0)} \simeq \frac{(E_0 - \Delta E_9 + m)^2 - m^2}{(E_0 - \Delta E_{10} + m)^2 - m^2} \frac{\phi_{10}(E_0 - \Delta E_{10})}{\phi_9(E_0 - \Delta E_9)} \quad (5)$$

where m is the nucleon mass, and $\Delta E_{9,10}$ are the energies per nucleon lost by the two beryllium isotopes. Introducing the average energy loss

$$\langle \Delta E_0 \rangle = \frac{\Delta E_9 + \Delta E_{10}}{2} \simeq \frac{19}{45} eV \quad (6)$$

and the difference

$$\delta E_0 = \frac{\Delta E_9 - \Delta E_{10}}{2} \simeq \frac{1}{45} eV \quad (7)$$

(with V the effective heliospheric potential for the data taking period considered) and expanding in first order in δE_0 one obtains:

$$\frac{\phi_{10}^{(\text{LIS})}(E_0 + \langle \Delta E_0 \rangle)}{\phi_9^{(\text{LIS})}(E_0 + \langle \Delta E_0 \rangle)} \simeq \frac{\phi_{10}^{\oplus}(E_0)}{\phi_9^{\oplus}(E_0)} \left\{ 1 - \left[\gamma_9(E_0) + \gamma_{10}(E_0) + \frac{4(E_0 + m)}{(E_0 + 2m)} \right] \frac{\delta E_0}{E_0} \right\}. \quad (8)$$

where $\gamma_A(E_0) = -d \ln \phi_A / d \ln E_0$ is the spectral index for the beryllium isotope with mass number A at the energy E_0 . Equation (8) states that the isotopic ratio in the LIS at the energy E'_0 can be obtained using the ratio observed at the Earth at the lower energy $E_0 = E'_0 - \langle \Delta E_0 \rangle$ and applying a correction factor to take into account for the different distortions suffered by the two spectra traversing the heliosphere. The beryllium spectra in the range measured by AMS02 decrease with energy, and therefore $\gamma_{9,10} > 0$, and the correction factor is ≤ 1 , reflecting the fact that for the lighter isotope Be9 the energy loss per nucleon in the heliosphere is larger, and the effects of modulations more important. For an effective heliospheric potential of order 0.5–0.6 GV as indicated by the data the correction factor is of order 0.9 for $E_0 \simeq 0.5$ GeV, growing monotonically with energy and approaching asymptotically unity (for $E_0 \gtrsim 30$ GeV). It should be noted that using this correction the isotopic ratio in the LIS grows with energy more rapidly than what is observed near the Earth.

C. Isotopic ratio at injection

To estimate the average survival probability from the isotopic ratio, we will make the simplifying assumption that the energy of the beryllium nuclei remains approximately constant during propagation. The average survival probability can then be written as:

$$P_{\text{surv}}(E_0) = \left[\frac{\phi_{10}(E_0)}{\phi_9(E_0)} \right] \times \left[\frac{\phi_9(E_0)}{\phi_{10}^{(0)}(E_0)} \right] \simeq \left[\frac{\phi_{10}(E_0)}{\phi_9(E_0)} \right] \times \left\{ \frac{\langle q_9(E_0) \rangle}{\langle q_{10}(E_0) \rangle} \times \frac{\mathcal{P}_{10}(E_0)}{\mathcal{P}_9(E_0)} \right\}. \quad (9)$$

In the first equality the probability is written as the product of the isotopic ratio (in the LIS), times a factor that takes into account for the difference in flux between the two isotopes, estimated assuming that also the Be10 isotope is stable. This correction factor is written in the second equality as the product of two sub-factors that take into account for differences in the injection rate and in the propagation for the two isotopes.

To estimate the correction factor associated with injection, it is safe to assume that all beryllium isotopes are generated by the same mechanism, that is the fragmentation of larger mass nuclei (mostly carbon and oxygen) in collision with target gas, therefore the injection rate for nuclei of type j can be written as:

$$q_j(E_0, \vec{x}, t) = 4\pi \beta c \sum_i n_i(\vec{x}) \sum_{k>j} \phi_k(E_0, \vec{x}, t) \sigma_{k+i \rightarrow j}(E_0) \quad (10)$$

where n_i is the density of target particles of type i in the medium where the particles are propagating, ϕ_k the flux of CR nuclei of type k , and $\sigma_{k+i \rightarrow j}$ the relevant fragmentation cross section. In these collisions the energy per nucleon of the projectile nucleus and of its fragments in the final state are approximately equal, and this is why it is convenient to study the spectra in terms of this kinematical variable.

Eq. (10) implies that the injection rates of different isotopes have essentially the same space and time distributions, and that their ratio in good approximation is only determined by nuclear fragmentation cross section. This follows from the fact that the composition of the target gas is expected to be approximately the same in the entire Galaxy, and that the relative abundances of different primary CR fluxes are expected to be close to what is observed locally, while the absolute values of the target gas density and of the primary spectra cancel in the ratio.

Uncertainties on the values of the fragmentation cross sections are however not negligible. Fig. 2 shows the ratio $q_{10}(E_0)/q_9(E_0)$ calculated using for the primary CR fluxes the carbon, nitrogen and oxygen spectra measured by AMS02 (deconvolving solar modulations with the FFA approximations), and two parametrizations of the proton–nucleus fragmentation cross sections. One parametrization is presented in Evoli et al. in [8], while the other is taken from the numerical code GALPROP [9–11].

Both models predict constant cross sections at high energy ($E_0 \gtrsim 10$ GeV), and therefore an approximately constant ratio of the injection rates, however for the Evoli et al. model this constant is of order 0.82, while using the GALPROP cross section the asymptotic ratio is of order 0.60. Important to note is also the energy dependence of the ratio. that for the Evoli et al. model grows slowly but monotonically from $\simeq 0.53$ at $E_0 = 0.5$ GeV to $\simeq 0.81$ for $E_0 \gtrsim 10$ GeV, while for the GALPROP model the injection ratio grows to a maximum $\simeq 0.66$ for $E_0 \approx 1.25$ GeV, and then decreases taking the asymptotic value ($\simeq 0.60$) for $E_0 > 5$ GeV.

The second factor in Eq. (10) takes into account the fact that (even neglecting decay) the propagations of different isotopes with the same energy per nucleon E_0 are not identical. This difference emerges because the isotopes have different rigidities, and therefore travel along different trajectories in a magnetic field, and they also have different absorption cross sections for collisions with interstellar gas. The size of the propagation effects is model dependent, but one can estimate that the ratio $\mathcal{P}_{10}/\mathcal{P}_9$ is close to unity (and a in fact a little less than unity).

The magnetic rigidities of isotopes of the same element with the same energy per nucleon are proportional to the mass number A , so the rigidity of Be10 nuclei is higher by a factor 10/9 with respect to Be9, and this is expected to result in a faster escape from the Galaxy. The rigidity dependence of this effect is often modelled as of power law form ($\propto \rho^{-\delta}$) with the exponent δ of order 0.3–0.5, so that the ratio of the propagation effects is of order 0.95–0.97. In other models the rigidity dependence of the escape is weaker, and the factor closer to unity.

The absorption cross section is larger for the higher mass number isotope, so that the effect is again to reduce the $\mathcal{P}_{10}/\mathcal{P}_9$ ratio, however the larger mass number A is compensated by the fact that in the beryllium–10 nucleus the space distribution of the nucleons is more compact, with an electromagnetic radius $\sqrt{\langle r^2 \rangle} \simeq 2.355$ fm (2.519 fm for Be9), the net result is that the difference in cross sections is small (of order few percent). In the following we will assume for the propagation correction factor $\mathcal{P}_{10}/\mathcal{P}_9$ a value of unity, and estimate that this could be an underestimate of only few percent.

Fig. 3 shows an estimate of the average survival probability obtained from the isotopic ratios measured by AMS02 and ISOMAX correcting for solar modulations (for the FFA potential $V = 0.5$ GV) and for the difference in injection rates using the parametrisation of the fragmentation cross sections of Evoli et al. [8] and of GALPROP [11]. Use of the two models results in some non negligible differences.

III. THE COSMIC RAY AGE DISTRIBUTION

The problem we will consider now is to interpret a measurement of the average survival probability in terms of CR propagation parameters. Naively, one could estimate an average age for the cosmic ray particles $\langle t_{\text{age}} \rangle$ using the simple expression:

$$P_{\text{surv}}(E_0) \simeq \exp \left[-\frac{\langle t_{\text{age}}(E_0) \rangle}{T_{\text{dec}}(E_0)} \right], \quad (11)$$

(with $T_{\text{dec}}(E_0)$ the decay time at the energy considered). This simple equation will however give in general incorrect results. The problem is that the CR particles observed near the solar system have been injected in interstellar space at different points and at different times, and therefore their age (that is the

time interval elapsed between injection and observation) is expected to have a broad distribution. The survival probability must then be obtained calculating the integral:

$$P_{\text{surv}}(E_0) = \int_0^\infty dt f_{\text{age}}(t, E_0) e^{-t/T_{\text{dec}}(E_0)} . \quad (12)$$

where $f_{\text{age}}(t, E_0)$ is the (normalised) age distribution (calculated neglecting the effect of decay). It is then manifest that the survival probability is determined by the *shape* of the age distribution and not only by a single parameter such as the average $\langle t_{\text{age}} \rangle$. The problem is then to construct a model for the age distribution.

A. The “leaky box model”

The “leaky box” model has been in use for several decades to describe CR propagation in the Galaxy. Because of its great simplicity the model is not really adequate to interpret current observations, however it can be instructive to consider here its predictions to illustrate some general points. The model neglects the space dependence of the cosmic ray spectra, and describes only a single energy spectrum for each particle type. Assuming that the energy of the CR particles remain constant during propagation, the stationary solution spectrum for an unstable particle is obtained solving the equation:

$$0 = \frac{dN}{dt} = Q - N \left[\frac{1}{T_{\text{esc}}} + \frac{1}{T_{\text{int}}} + \frac{1}{T_{\text{dec}}} \right] = Q - \frac{N}{T_{\text{esc}}} (1 + r + \tau) \quad (13)$$

(where we have left implicit the energy dependence) that is determined by the three characteristic times for escape, interaction and decay. Eq. (13) is constructed assuming that the age distribution of the particles, neglecting the effects of interactions, is a simple exponential with slope T_{esc} . In the last equality of Eq. (13) we have introduced the notations $r = T_{\text{esc}}/T_{\text{int}}$ and $\tau = T_{\text{esc}}/T_{\text{dec}}$. The three mechanism of escape, interactions and decay all contribute to the losses of CR particles, and the probabilities for a CR particle to escape, interact or decay are given by: $1/(1 + r + \tau)$, $r/(1 + r + \tau)$ and $\tau/(1 + r + \tau)$.

The average survival probability discussed in this paper can be obtained comparing spectra calculated including and neglecting decay and is:

$$P_{\text{surv}}^{(\text{l.b.})} = \frac{1 + r}{1 + r + \tau} = \frac{1 + \tau s}{1 + \tau(1 + s)} \quad (14)$$

where we have also introduced the adimensional parameter: $s = r\tau = T_{\text{dec}}/T_{\text{int}}$. The average survival probability (for fixed values of T_{dec} and T_{int}) decreases monotonically for increasing τ (or equivalently T_{esc}), being unity for short escape times, and reaching a finite asymptotic value for large τ (or $T_{\text{esc}} \rightarrow \infty$):

$$\lim_{T_{\text{esc}} \rightarrow \infty} P_{\text{surv}}^{(\text{l.b.})} = \frac{s}{1 + s} = \frac{T_{\text{dec}}}{T_{\text{dec}} + T_{\text{int}}} . \quad (15)$$

Using the leaky box model to interpret the measurement $P_{\text{surv}}(E_0) = P$ and estimate the escape time, one obtains an infinite number of solutions that can be parametrised with the assumed value for the interaction time T_{int} :

$$T_{\text{esc}} = T_{\text{dec}} \frac{1 - P}{P - (1 - P)s} \quad (16)$$

and span the interval:

$$T_{\text{dec}} (1/P - 1) \leq T_{\text{esc}} < \infty . \quad (17)$$

The shortest estimate for T_{esc} corresponds to a very long (diverging) interaction time, that is to propagation in a very low density medium where interactions are negligible. Longer values of T_{esc} correspond

to shorter interaction times, and a divergent value of T_{esc} corresponds to a shortest possible value of the interaction time [$T_{\text{int}} = T_{\text{dec}} (1/P - 1)$], and therefore to an upper limit for the density of the CR propagation medium:

$$n_{\text{ism}} \leq \frac{1}{(\sigma_{\text{abs}} \beta c T_{\text{dec}})} \left(\frac{1}{P} - 1 \right) \quad (18)$$

(with σ_{abs} the absorption cross section).

The simple results discussed above, that a measurement of the average survival probability correspond to a lower limit for the CR age, and to an upper limit on the average density of the propagation medium remain valid also for the much better motivated diffusion models discussed below.

B. Diffusion Models

The construction of CR Galactic propagation models has been a central problem in the field for more than seven decades, and several authors have discussed models where the effects of the interstellar magnetic fields are described in terms of diffusion. The first diffusion model was in fact introduced already in 1951 by Giuseppe Cocconi [12], who developed the ideas introduced by Enrico Fermi, who first proposed a Galactic origin for cosmic rays [13], allowing for the possibility that the CR particles are not permanently confined by the Galactic magnetic fields, but can be lost “partly destroyed by collisions with interstellar matter and partly by diffusing out of the Galaxy”. To model CR escape, Cocconi described the Galaxy as a homogeneous sphere of radius R with a stationary source at the center, and propagation as isotropic diffusion with a constant (and implicitly energy independent) diffusion coefficient. Using the boundary condition that the CR density vanishes at the border of the Galaxy, Cocconi could then compute the power required to generate the observed CR density at the Earth.

These concepts were developed further by Morrison, Olbert and Rossi [14], who improved on the spherical model of Cocconi assuming a cylindrical Galactic confinement volume and more realistic space distributions of the CR sources calculating stationary solutions of the diffusion equation, assuming again a homogeneous, isotropic diffusion coefficient, and the boundary condition that the CR density vanishes at the outer limits of the confinement volume.

The framework where magnetic propagation in the Galaxy is described as diffusion has been later extensively discussed, with the inclusion of other effects, such as energy losses, interactions, advection and decay, in the influential textbook by Ginzburg and Syrovatskii [15]. This description of propagation has incorporated into numerical codes such as GALPROP [9–11], DRAGON [16, 17], USINE [18] and PICARD [19]. There is at present a large body of literature that interprets the measurements of the CR spectra with models based on diffusion.

IV. THE “MINIMAL DIFFUSION MODEL”

In this paper we will consider the simplest possible version diffusion model. In this model we will assume that the energy of the CR particles remain constant after injection, and propagation is described as isotropic diffusion with a constant diffusion coefficient D (of arbitrary energy dependence) in the volume (the “halo”) between the two planes $z \pm Z_{\text{halo}}$ that act as absorbers. Particle are injected continuously in space and time from the “disk” volume between the planes $z = \pm Z_{\text{disk}}$ with a constant rate q . The disk volume is homogeneously filled with gas of number density n_{disk} , while the gas density in the region $|z| > Z_{\text{disk}}$ vanishes. The absorption cross section (averaged over the composition of the target gas) is σ_{abs} , and the particles can also decay with characteristic time T_{dec} . The observation point where the CR spectrum is measured has the vertical coordinate z_{obs} . The model is therefore defined by the set of eight parameters q , z_{obs} , Z_{disk} , n_{disk} , σ_{abs} , T_{dec} , Z_{halo} and D . We find convenient to introduce the diffusion time

$$T_{\text{diff}} = \frac{Z_{\text{halo}}^2}{2D} \quad (19)$$

that gives the order of magnitude of the CR Galactic residence time, and to discuss the results of the model replacing the diffusion coefficient D with the diffusion time T_{diff} .

Of the eight parameters of the model, the injection rate controls the absolute normalisation of the observed spectrum and cancels in the expressions for the survival probability. Three parameters (z_{obs} , Z_{disk} and n_{disk}) must be estimated from astrophysical observations of the structure of the Galaxy. The solar system is very close to the Galactic plane and we will assume $z_{\text{obs}} = 0$. In the numerical work performed below we will also use $Z_{\text{disk}} \simeq 0.15$ kpc and $n_{\text{disk}} \simeq 1 \text{ cm}^{-3}$ with a composition (following Ferriere [20]) formed by 0.9 hydrogen, 0.0875 helium and 0.0125 metals.

The absorption cross section can be in principle measured from laboratory experiments, or calculated using Glauber models from a knowledge of the pp cross sections. We performed such calculation and obtain for Be10 collisions with hydrogen, helium and oxygen nuclei at kinetic energy $E_0 \simeq 5$ GeV (and including fragmentation reactions without pion production) cross sections of 234, 529 and 1051 mbarn. with only a weak energy dependence. This corresponds to an average cross sections of order 270 mbarn (with a weak energy dependence) and an interaction time for propagation in the disk:

$$T_{\text{int}}^{\text{disk}} = [\beta c \sigma_{\text{abs}} n_{\text{disk}}]^{-1} \simeq 3.92 \beta \left[\frac{1 \text{ cm}^{-3}}{n_{\text{disk}}} \right] \left[\frac{270 \text{ mbarn}}{\sigma_{\text{abs}}} \right] \text{ Myr} \quad (20)$$

The decay time is readily obtained including relativistic effects:

$$T_{\text{dec}}(E_0) \simeq 2.001 (1 + 1.073 E_0) \text{ Myr} \quad (21)$$

(with E_0 the kinetic energy per nucleon in GeV). One can note that the decay and interaction time can be of comparable length, and therefore that it is important to consider carefully how they contribute to the formation of the CR spectra of unstable particles.

The free parameters of model that must be determined from observations of CR properties are then the diffusion time T_{diff} and the halo size Z_{halo} .

The motivation for using this very simple model is that it captures the main properties (and possess the main limitations) of more complicated models, but it is sufficiently simple to allow to obtain exact analytic solutions for several interesting quantities, including the average survival probability, and this can be very valuable to develop an understanding of the problem.

A. Escape time and age distributions

In the leaky box model, discussed in the previous section, the quantity T_{esc} is equal (neglecting interactions) to both the average escape time from the Galaxy and the average age, that is time elapsed from injection to observation for the CR particles. In more realistic models these two quantities (escape time and age) do not coincide, and are also not uniquely defined, because the first one depends on the injection point, and the second one depends on the observation point.

In the Minimal Diffusion Model, if interactions are neglected, it is straightforward to calculate (in the form of a series) the distributions for both characteristic times (see [1]). Some examples of the escape time distributions are shown in Fig. 4. The average $\langle t_{\text{esc}} \rangle$ can be calculated exactly, and is:

$$\langle t_{\text{esc}}(z_s) \rangle = T_{\text{diff}} \left(1 - \frac{z_s^2}{Z_{\text{halo}}^2} \right) \quad (22)$$

(with z_s the vertical coordinate of the injection point), a result that clarifies the physical meaning associated to the diffusion time.

The average age is a function of the observation point, but also on the space and time distributions of the injection. For an injection that is constant in time and continuous in space in the volume $|z| \leq Z_{\text{disk}}$, the age distribution, neglecting interactions, has been calculated in [1], and some examples are shown in Fig. 5. The average age is proportional to T_{diff} , and depends on on the vertical coordinate of the observation point, and on the ratio $Z_{\text{disk}}/Z_{\text{halo}}$. For an observation point on the Galactic disk ($z_{\text{obs}} = 0$)

one has:

$$\langle t_{\text{age}}(z_{\text{obs}} = 0, \sigma_{\text{abs}} = 0) \rangle = T_{\text{diff}} \frac{2}{3} \left[1 + \frac{h}{2} - \frac{h^2}{4} \right] \quad (23)$$

(with $h = Z_{\text{disk}}/Z_{\text{halo}}$). Therefore the average age is of the same order, but not identical to the average escape time.

Including the effects of interactions the average age decreases because long trajectories suffer more absorption, and their contribution is suppressed. A general expression of $\langle t_{\text{age}} \rangle$ valid for an arbitrary observation point and any value of the ratio h and of the absorption cross section can be obtained, but is not given here because it is rather complicated. The simple expression valid for the interesting case of a small h and $z_{\text{obs}} = 0$ is:

$$\langle t_{\text{age}}(z_{\text{obs}} = 0, h \rightarrow 0) \rangle = T_{\text{diff}} \frac{2}{3 + 6r} \quad (24)$$

where the adimensional quantity r :

$$r = \beta c T_{\text{diff}} \sigma_{\text{abs}} n_{\text{disk}} h \quad (25)$$

has the simple physical meaning of the the average number of interactions during a diffusion time, calculated after diluting uniformly the interstellar gas in the entire confinement volume.

An interesting quantity is the average column density (or grammage) crossed by the CR particles. Neglecting the effect of interactions, and for $z_{\text{obs}} = 0$, one has:

$$\langle X \rangle = m \beta c T_{\text{diff}} n_{\text{disk}} \frac{4h}{2-h} \left(1 - \frac{7}{6}h + \frac{3}{8}h^2 \right) = X_{\text{disk}} \frac{\beta c T_{\text{diff}}}{Z_{\text{halo}}} \frac{2}{2-h} \left(1 - \frac{7}{6}h + \frac{3}{8}h^2 \right) \quad (26)$$

(where m is the average mass of nuclei in the interstellar gas, and $X_{\text{disk}} = 2 Z_{\text{disk}} n_{\text{disk}} m$ is the vertical grammage of the disk). Dividing this grammage by the average age given in Eq. (23) one finds that the observed CR particles have traveled in a medium of average density

$$\langle n_{\text{traj}} \rangle = n_{\text{disk}} 3h \frac{2}{(2-h)} \left(\frac{1 - 7/6 h + 3/8 h^2}{1 - 1/2 h + 1/4 h^2} \right) \simeq n_{\text{disk}} 3h \left(1 - \frac{7}{6}h + \frac{21}{24}h^2 + \dots \right) \quad (27)$$

This equation states that for small h (that is for $Z_{\text{halo}} \gg Z_{\text{disk}}$) the CR particles have traveled in a medium with an average density that is three times what is obtained diluting uniformly the gas in the entire halo volume.

It is important to note that Eq. (27) gives a global average, and trajectories of different length encounter different average densities. All particles have their origin and are observed inside the Galactic disk, therefore for very short trajectories the average density is $\langle n_{\text{ism}} \rangle \simeq n_{\text{disk}}$, increasing the length of the trajectory, the average density decreases monotonically.

The average survival probability depends not only on the average age of the CR particles, but also on the shape of the age distribution. This shape, for the case where interactions are negligible, has already been discussed in [1] and has the scaling form:

$$f_{\text{age}}(t) = \frac{1}{T_{\text{diff}}} F_{\text{age}} \left(\frac{t}{T_{\text{diff}}}, \frac{Z_{\text{disk}}}{Z_{\text{halo}}}, \frac{z_{\text{obs}}}{Z_{\text{halo}}} \right) \quad (28)$$

and depends only on adimensional ratios.

Examples of the distributions, for an observation point with $z_{\text{obs}} = 0$, are shown in Fig. 5 for three values of the ratio $h = Z_{\text{disk}}/Z_{\text{halo}}$. Inspecting the figure one can easily see the main features of the age distribution that can be summarised writing:

$$f_{\text{age}}(t) \propto \begin{cases} \text{const.} & \text{for } t \lesssim T_{\text{diff}} h^2, \\ t^{-1/2} & \text{for } h^2 \lesssim t/T_{\text{diff}} \lesssim 1, \\ e^{-t/T^*} & \text{for } t \gtrsim T_{\text{diff}} \quad (\text{with } T^* = 8/\pi^2 T_{\text{diff}}). \end{cases} \quad (29)$$

One can therefore identify three ranges of t where the distributions has different forms. For long times ($t \gtrsim T_{\text{diff}}$) the distribution has an exponential shape, with slope $T^* = 8/\pi^2 T_{\text{diff}}$. In the range $h^2 \lesssim t/T_{\text{diff}} \lesssim 1$ the distribution grows rapidly for shorter times $\propto t^{-1/2}$. Finally, for very short times ($t/T_{\text{diff}} \lesssim h^2$) the distribution becomes a constant.

For the limiting cases $h = 1$ and $h \rightarrow 0$ the asymptotic forms (for short and long times) of the age distributions have simple expressions. For $h = 1$ one has:

$$F_{\text{age}}^{(h=1)}(x) \simeq \begin{cases} 1 & \text{for } x \lesssim 0.5 \\ \frac{4}{\pi} \exp\left[-\frac{\pi^2}{8} x\right] & \text{for } x \gtrsim 0.5, \end{cases} \quad (30)$$

for $h = 0$:

$$F_{\text{age}}^{(h=0)}(x) \simeq \begin{cases} 1/\sqrt{2\pi x} & \text{for } x \lesssim 0.5 \\ \exp\left[-\frac{\pi^2}{8} x\right] & \text{for } x \gtrsim 0.5 \end{cases} \quad (31)$$

In Eqs. (30) and (31) (where $x = t/T_{\text{diff}}$) the expressions are exact asymptotically, in the limits of small and large x , but are also a good approximation (better than 10%) of the correct result in the entire x range.

B. Average survival probability for a purely magnetic propagation

It is straightforward to calculate the average survival probability for the case of a purely magnetic propagation, that is neglecting the effect of interactions [1]. The result can be expressed in terms of the adimensional parameters $\tau = T_{\text{diff}}/T_{\text{dec}}$ and $h = Z_{\text{disk}}/Z_{\text{halo}}$:

$$P_{\text{surv}}^{\text{no int.}}(\tau, h) = \frac{1 - \cosh[\sqrt{2\tau}(1-h)] (\cosh[\sqrt{2\tau}])^{-1}}{\tau h(2-h)}. \quad (32)$$

For the limiting cases $h = 1$, and $h = 0$ one has:

$$P_{\text{surv}}^{\text{no int.}}(\tau, h = 1) = \frac{1}{\tau} \left(1 - \frac{1}{\cosh[\sqrt{2\tau}]} \right) \simeq \frac{1}{1 + \tau} \quad (33)$$

$$P_{\text{surv}}^{\text{no int.}}(\tau, h = 0) = \frac{\tanh[\sqrt{2\tau}]}{\sqrt{2\tau}} \simeq \frac{1}{\sqrt{1 + 2\tau}} \quad (34)$$

In these equations first equality is an exact result, while the second (approximate) one gives a simpler analytic forms that has the correct asymptotic behaviours for large and small τ and differ from the correct expressions by less that 10% in the entire range of definition. It is elementary to derive the simple expressions for the survival probability from the expressions for the age distribution given in Eqs. (30) and (31).

One can note that the case $h = 1$ when the confinement and source volume coincide the age distribution is essentially indistinguishable from the ‘‘leaky box’’ model, while for small h the age distribution has a large contribution of short times and for $T_{\text{diff}}/T_{\text{dec}}$ small the survival probability is much larger than the leaky box model prediction.

The approximate forms for the average survival probability given in Eqs. (30) and (31) can be inverted, so that a measurement $P_{\text{surv}} = P$ can translated into a diffusion time with closed form expressions:

$$T_{\text{diff}}(h = 1) = T_{\text{dec}} \left(\frac{1}{P} - 1 \right) \quad (35)$$

$$T_{\text{diff}}(h = 0) = T_{\text{dec}} \frac{1}{2} \left(\frac{1}{P^2} - 1 \right) \quad (36)$$

These results can be compared to the estimate of the age obtained with the assumption that the distribution is narrow and centered at the value T_{age} :

$$T_{\text{age}} \simeq T_{\text{dec}} (-\ln P) . \quad (37)$$

These results (also shown in Fig. 6) illustrate how the estimate of the age is strongly model dependent.

The relation between the age distribution and the average survival probability is illustrated in Fig. 7 that shows one example of the age distribution and the effects of decay on the distribution for two values of T_{dec} . In the figure the value of the survival probability can be easily visualised as the ratio of the areas below the curves that include and neglect decay.

As already stated, the age distribution, and therefore the average survival probability, depends on the space and time distributions of the injection. The results obtained in this section have been calculated assuming an injection continuous in time and space, as it is the case when the main source of beryllium nuclei is the fragmentation of primary cosmic rays in interstellar space. An alternative possibility [30–36] is that the nuclei are generated by collisions inside or in the vicinity of CR accelerators. In this case the injection is not continuous, because the accelerators are very likely discrete and transient astrophysical objects, active for only a short time. In this scenario it is also not possible to make a unique prediction for the properties of the injection, in part because the CR accelerators have not been firmly identified, and also because the sources are of stochastic nature, and one can only predict their average properties, and the contribution to the observable spectrum of short age particles, generated by very near and very young sources can have very large fluctuations.

This problem is illustrated in Fig. 8, where the continuous line is the age distribution calculated for a continuous (in space and time) injection, while the histogram is one realisation of a discrete source model generated with Montecarlo methods assuming that the injection is formed by a set of discrete, instantaneous emissions with a rate of one per century in one disk of radius 15 Kpc (a choice motivated by the properties of Supernova remnants). This injection model is constructed so that the *average* of the age distributions obtained from different realisations of the ensemble of sources is identical to the previous (continuous injection) case. For the Montecarlo realisation of the sources shown in the figure the contribution of very short ages (associated to young near accelerator events) is reduced with respect to the prediction of a continuous injection, and using Eq. (32) to estimate the diffusion time from the average survival probability results in an overestimate of the correct diffusion time of order 4-5%.

If the injection of the beryllium nuclei is generated in sources, their stochastic nature will be a source of systematic uncertainty. If the distribution of the sources has the same statistical properties of Supernova explosions, the approximation of assuming a continuous injection results in most cases to an underestimate of the diffusion time of order of few percent, because only in rare cases one finds a very young source event in the vicinity of the solar system.

C. Average survival probability including interactions

The effects of interactions on the average survival probability can be significant if the CR confinement volume is not too large. For a stationary continuous injection one can obtain explicit analytic expressions for the average survival probability that can be written as a function of the adimensional parameters τ , h and s :

$$s = s_{\text{disk}} h = \frac{T_{\text{dec}} h}{T_{\text{int}}^{\text{disk}}} = \beta c T_{\text{dec}} n_{\text{disk}} \sigma_{\text{abs}} \frac{Z_{\text{disk}}}{Z_{\text{halo}}} . \quad (38)$$

The parameter s has the simple physical meaning of the average number of interactions during a decay time calculated diluting uniformly the interstellar gas in the entire Galactic volume, while $s_{\text{disk}} = s/h$ is the same quantity for particles propagating only in the disk.

For an observation point on the Galactic plane, the average survival probability, including the effects of interactions takes the form:

$$P_{\text{surv}}(\tau, h, s) = \frac{s}{h + s} \frac{e^{\sqrt{2h(h+s)\tau} - 1}}{e^{\sqrt{2hs\tau} - 1}} \frac{A_1 B_1}{A_2 B_2} \quad (39)$$

where $A_{1,2}$ and $B_{1,2}$ are:

$$\begin{aligned}
A_1 &= e^{\sqrt{2\tau}h(2+\sqrt{(h+s)/h})}(\sqrt{h}-\sqrt{h+s})-e^{2\sqrt{2\tau}}(\sqrt{h+s}-\sqrt{h}) \\
A_2 &= e^{\sqrt{2\tau}h(2+\sqrt{h(h+s)})}(\sqrt{h}+\sqrt{h+s})+e^{2h\sqrt{2\tau}}(\sqrt{h+s}+\sqrt{h}) \\
B_1 &= +\sqrt{(2s\tau)/h}(1-h)-e^{2\sqrt{2hs\tau}}\left(1+\sqrt{(2s\tau)/h}(1-h)\right)-1 \\
B_2 &= -\sqrt{(2s\tau)/h}(1-h)-e^{\sqrt{2hs\tau}}\left(1+\sqrt{(2s\tau)/h}(1-h)\right)+1
\end{aligned}$$

The limit of the survival probability for a very short diffusion time is (obviously):

$$\lim_{\tau \rightarrow 0} P_{\text{surv}}(\tau, s, h) = 1, \quad (40)$$

the opposite limit, for very long diffusion times is:

$$\lim_{\tau \rightarrow \infty} P_{\text{surv}}(\tau, s, h) = \frac{s}{s+h} = \frac{s_{\text{disk}}}{s_{\text{disk}}+1} \quad (41)$$

This result can be understood noting that for very slow diffusion (very long T_{diff}) the CR particles remain always confined in the Galactic disk where they decay or interact (with a negligible escape probability). The average survival probability is then controlled by the relative importance of decay and interaction in the disk region.

Some examples of the survival probability with the inclusion of the effects of interactions are shown in Fig. 9. Inspecting the figure one can see that in general the survival probability has the limits given in Eqs. (40) and (41), with one minimum. The existence of this minimum can be easily understood, and it corresponds to a diffusion time that is sufficiently long to have a large decay probability, but not too long, because the particles must be able to diffuse out of the disk before being absorbed, and spend time in the region of the halo where the target density is low and decay is favored over interactions. The minimum decay probability can be well below the asymptotic value of Eq. (41).

The Minimum in the survival probability is absent for the case $h = 1$, when the average survival probability takes the form:

$$P_{\text{surv}}(\tau, h = 1, s) = \frac{s}{s+1} \frac{(e^{2\sqrt{2s\tau}} + 1)(e^{\sqrt{2(1+s)\tau}} - 1)^2}{(e^{\sqrt{2(1+s)\tau}} + 1)(e^{\sqrt{2s\tau}} - 1)^2} \quad (42)$$

that can be obtained simply substituting the value $h = 1$ in Eq. (39). In this case the probability decreases monotonically from unity at $\tau = 0$ to the asymptotic value $s/(1+s)$ for $\tau = \infty$. This result, shown in Fig. 10 is numerically very close to survival probability for the leaky box model Eq. (14).

The distribution in the limit ($h \rightarrow 0$) but for a constant value of the parameter s can be obtained keeping the halo size fixed, and sending $Z_{\text{disk}} \rightarrow 0$, but increasing n_{disk} so that the product $Z_{\text{disk}} n_{\text{disk}}$ is constant. The average survival probability then takes the form:

$$P_{\text{surv}}(\tau, h = 0, s) = \frac{(e^{2\sqrt{2\tau}} - 1)(1 + 2\tau s)}{(e^{2\sqrt{2\tau}} + 1)\sqrt{2\tau} + (e^{2\sqrt{2\tau}} - 1)2\tau s}. \quad (43)$$

This expression is a good approximation of the average survival probability for h small, except for τ much larger than the value τ^* where the probability has a minimum. This is because in the limit $\tau \rightarrow \infty$ the expression in Eq. (43) goes to unity, in agreement with Eq. (41) for a divergent gas density in the disk.

The interpretation of a measurement of the average survival probability for Be10 nuclei at kinetic energy per nucleon E_0

$$P_{\text{surv}}(E_0) = P \quad (44)$$

in the framework of the Simple Diffusion Model, is in general (without using other considerations) not unique because there is an infinite number solutions in the form of pair of values $\{Z_{\text{halo}}, T_{\text{diff}}\}$, with one quantity determining the other. The value of T_{diff} and Z_{halo} that are solutions of Eq. (44) are in the intervals:

$$\begin{cases} T_{\text{diff}}^{\min} \leq T_{\text{diff}} \leq T_{\text{diff}}^{\max} \\ Z_{\text{halo}}^{\min} \leq Z_{\text{halo}} < \infty \end{cases} \quad (45)$$

with the minimum diffusion time T_{diff}^{\min} corresponding to a divergent vertical halo size, and the maximum T_{diff}^{\max} corresponding to the smallest halo size Z_{halo}^{\min} .

An illustration of how a measurement of P_{surv} corresponds to allowed intervals for T_{diff} and Z_{halo} is shown in Fig. 11. The example shown in the figure corresponds to a measurement $P_{\text{surv}} = 0.285$ obtained for $E_0 = 1.57$ GeV/n. The lower limit for T_{diff} corresponds to a very large halo size and to a situation where interactions are negligible. In this case the average survival probability takes the form of Eq. (34), and using the approximate form of the probability in the second equality in Eq. (34) one obtains the simple expression

$$T_{\text{diff}}^{\min}(P) \simeq T_{\text{dec}} \frac{1}{2} \left(\frac{1}{P^2} - 1 \right) \quad (46)$$

Inspecting Fig. 11, it is easy to see that the maximum value of the diffusion time $T_{\text{diff}}^{\max}(P)$ and the corresponding minimum value of the vertical halo size $Z_{\text{halo}}^{\min}(P)$ can be calculated from the condition that the survival probability has a minimum for $T_{\text{diff}} = T_{\text{diff}}^{\max}(P)$. This corresponds to solving the system of two equations:

$$\begin{cases} P_{\text{surv}} \left(\tau^* = \frac{T_{\text{diff}}^{\max}}{T_{\text{dec}}}, h^* = \frac{Z_{\text{disk}}}{Z_{\text{halo}}^{\min}}, s^* = s_{\text{disk}} \frac{Z_{\text{disk}}}{Z_{\text{halo}}^{\min}} \right) = P \\ dP_{\text{surv}}/d\tau(\tau^*, h^*, s^*) = 0. \end{cases} \quad (47)$$

It is straightforward to solve numerically Eq. (47) to obtain the maximum diffusion time $T_{\text{diff}}^*(P)$ and the minimum halo size Z_{halo}^* that corresponds to a survival probability P . It is however also possible to have an explicit solution that is a reasonably good approximation when $Z_{\text{disk}}/Z_{\text{halo}}^{\min}$ is small (that is in fact the case for the real data). In this limit the average survival probability can be described by the expression in Eq. (43), and the position of the minimum (τ^*), and the value of the probability at the minimum (P_{surv}^*) can be then expressed as a function of the parameter s . The results are reasonably well represented by the analytic expressions:

$$\tau^*(s) \simeq 2 \sqrt{\frac{1}{16(\sqrt{s(s+1)} - s)^4} - 1} \quad (48)$$

and

$$P_{\text{surv}}^*(s) = P_{\text{surv}}(\tau^*, h = 0, s) \simeq 2 \sqrt{\frac{s}{1+4s}} \quad (49)$$

The line in the plane $\{\tau, P_{\text{surv}}\}$ described by the parametric form $\{\tau^*(s), P^*(s)\}$ is shown as a red dotted line in Fig. 9 and (to a very good approximation) corresponds to the set of minima for the curves $P_{\text{surv}}(\tau, h \simeq 0, s)$ for all values of s . Inverting Eq. (49) the parameter s can be expressed as a function of P :

$$s^*(P) \simeq \frac{P^2}{4(P-1)} \quad (50)$$

and this s value can be inserted in Eqs. (48) and (38) to obtain explicit expressions for the maximum diffusion time and minimum halo size:

$$\begin{cases} T_{\text{diff}}^{\max}(P) = T_{\text{dec}} \tau^*(P) \simeq T_{\text{dec}} 2 \sqrt{\frac{1}{P^4} - 1}, \\ Z_{\text{halo}}^{\min}(P) \simeq Z_{\text{disk}} [\beta c T_{\text{dec}} \sigma_{\text{abs}} n_{\text{disk}}] \frac{P^2}{4(P-1)}. \end{cases} \quad (51)$$

V. INTERPRETATION OF THE AMS02 BERYLLIUM MEASUREMENT

It can be interesting to study the average survival probabilities for Be10 nuclei inferred from the preliminary AMS02 measurement of the beryllium isotopic composition in the framework of the Minimal Diffusion Model discussed in the previous section.

Two examples of this exercise are given in Fig. 12 that shows (as shaded area) the allowed regions in the plane $\{Z_{\text{halo}}, T_{\text{diff}}\}$ obtained finding all solutions of the equation:

$$P_{\text{surv}} \left(\tau = \frac{T_{\text{diff}}}{T_{\text{dec}}(E_0)}, h = \frac{Z_{\text{disk}}}{Z_{\text{halo}}}, s = s_{\text{disk}} \frac{Z_{\text{disk}}}{Z_{\text{halo}}} \right) = [P(E_0) \pm \Delta P(E_0)] \quad (52)$$

where $P(E_0) \pm \Delta P(E_0)$ is the estimate of the average survival probability obtained from the AMS02 measurement of the beryllium isotopic composition at kinetic energy per nucleon E_0 , and the probability $P_{\text{surv}}(\tau, h, s)$ (calculated in the framework of the Minimal Diffusion Model) is given by Eq. (39).

In Fig. 12 the top (bottom) panel shows the allowed region for the estimate at $E_0 \simeq 1.57$ GeV ($E_0 \simeq 9.59$ GeV) using the fragmentation cross sections in the GALPROP code. As discussed in the previous section, the measurement of the survival probability corresponds to an allowed interval of T_{diff} , with a lowest value that requires a very large halo size, and a maximum value that corresponds to the smallest possible halo.

The pair of parameters $\{Z_{\text{halo}}, T_{\text{diff}}\}$ determines the average grammage $\langle X \rangle$ traversed by secondary particles, [see Eq. (26)], and lines of constant $\langle X \rangle$ are also shown in the figure.

Fig. 13 shows a summary of the diffusion times estimated from the AMS02 measurements interpreted in the framework of the Minimal Diffusion Model. The top panel shows estimates of the allowed interval of T_{diff} calculated assuming a very large halo size, while the bottom panel shows the T_{diff} interval calculated for the smallest halo size consistent with the measurement. In both cases, for each energy the interval is calculated twice using the fragmentation cross sections of Evoli et al. [8] and of GALPROP [11]. For both cross section models, if one assumes a large confinement volume the diffusion time at $E_0 \simeq 1$ GeV is of order 30 Myr. Increasing the energy, for the GALPROP cross sections the diffusion time remains approximately constant, except for the two highest energy points ($E_0 \simeq 9.5$ – 11.5 GeV) where the estimate becomes a factor 2–3 higher. Using the Evoli et al. cross sections, that estimate a larger Be10 fraction at production, the effects of decay must be larger, and the diffusion time longer, so that T_{diff} is estimated of order 50–60 Myr when E_0 is a few GeV. The diffusion times estimated for the two highest energy points is large ($T_{\text{diff}} \gtrsim 100$ Myr).

Fig. 14 shows lower limits on the vertical halo size obtained with the two sets of fragmentation cross sections for different values of the energy. The limits are of order of 5 Kpc for $E_0 \approx 1$ – 2 GeV, and grow with increasing energy, being more stringent for the Evoli et al. cross sections.

VI. OUTLOOK

Several works on Galactic cosmic rays have estimated the properties of their propagation in the Milky Way from the study of the ratios of the spectra of secondary (Li, Be and B) and primary (C, O, ...) nuclei. This ratio can be interpreted in terms of the grammage traversed by the CR particles. For example the HEAO-3 team [21] used a leaky box model framework to estimate a rigidity dependent grammage: $\langle X \rangle \simeq 14.0 \beta (\mathcal{R}/\mathcal{R}_0)^{-0.60}$ for rigidities $\mathcal{R} > \mathcal{R}_0 = 4.4$ GV (and a constant value for $\mathcal{R} < \mathcal{R}_0$). More recently Evoli, Aloisio and Blasi [22] interpreted the AMS02 data in a diffusion model, obtaining results very close to those of the HEAO-3 collaboration ($\langle X \rangle \simeq 8.4$ g/cm² at $\mathcal{R} > 10$ GV, and a rigidity dependence $\propto \mathcal{R}^{-0.63}$). If one makes the assumption that the grammage is integrated during propagation in interstellar space, one can then infer the CR Galactic residence time, or more in general the product of the residence time and the average density of the interstellar medium along the CR trajectories. Several authors have recently discussed estimates of these quantities in the framework of diffusive models [23–29] obtaining results that are in reasonable (if not perfect) agreement with each other.

A very attractive and often discussed idea is to combine the studies of the secondary/primary ratio and of the beryllium isotopic composition to solve the ambiguity in the interpretation of the data between

confinement time and average density, and more in general to test the assumption that the grammage is integrated in interstellar space.

We will postpone a detailed discussion of such a combined study waiting for the publication of the beryllium isotopic composition measurements by the AMS collaboration. We can however note that the preliminary study performed here indicates that there is significant tension between the standard interpretation of the secondary/primary ratio and the estimates of the cosmic ray age inferred from the preliminary AMS02 data. The diffusion times calculated using the “Minimal Diffusion Model” appear to *increase* with energy, by a factor of order two to three, when the kinetic energy per nucleon grows from 1 to 10 GeV, in contrast to the results obtained from the primary/secondary ratio, that suggest that the diffusion time should decrease by a factor larger than two in the same energy interval.

The indications of a discrepancy are stronger (weaker) when the effects of decay are calculated using the nuclear fragmentation cross sections of Evoli et al. [8], (GALPROP [11]), and emerge especially from the two highest energy points of the AMS02 measurements. It is therefore possible that the apparent conflict between data and model is the result of incorrect estimates of the relevant nuclear cross sections, and/or of systematic errors in the preliminary data. It can however be interesting to speculate on the implications of the case where the results are confirmed, and the estimates of the fragmentation cross sections remain valid.

It should be noted that the possibility of a conflict between the data on the beryllium isotopic composition and the estimates of the cosmic ray age inferred by the secondary/primary ratios can be understood qualitatively with simple considerations. In the AMS02 the isotopic ratio Be10/Be9 grows slowly from $R \simeq 0.16$ – 0.17 for an observed energy E_0 of order 0.7–1.0 GeV (that corresponds to a energy of order 0.9–1.2 GeV outside the heliosphere), to $R \simeq 0.25$ for E_0 of order 4–6 GeV. The three highest energy points (at $E_0 \simeq 8, 9.5$ and 11.4 GeV) have values $R \simeq (0.31 \pm 0.03), (0.25 \pm 0.03)$ and (0.21 ± 0.04) . In this energy range the decay time T_{dec} grows by a factor larger than six, from 4.1 Myr at $E_0 = 1$ GeV to 25.6 Myr at 11 GeV, and therefore one expect that even if the CR age is energy independent, the size the effects of decay on the unstable Be10 isotope should decrease significantly. Moreover, the data on the secondary/primary ratio (in the standard interpretation) suggest that the CR age decrease as a power law with rigidity ($\langle t_{\text{age}} \rangle \propto \beta \mathcal{R}^{-\delta}$). The energy interval of the AMS02 data corresponds to the rigidity range $\mathcal{R} \simeq 4.2$ – 29.7 GV, resulting in an expected shortening of the CR average age by a factor that goes from 1.7 (for $\delta = 0.33$) to 2.3 (for $\delta = 0.5$) in the interval of the AMS02 measurements. The two effects, the longer decay time and the expected shorter residence time, both go in the direction of reducing the effects of decay, and therefore one expects the average survival probability to have a significant increase in the energy range of the AMS02 measurements.

The estimate of the average survival probability from the isotopic ratio depends on the nuclear fragmentation cross section, and therefore the slow energy dependence of the isotopic ratio could in principle be the result of a cancellation, with a Be10/Be9 ratio at production that grows with energy, and energy decay effects that are stronger at low energy. For the models of the fragmentation cross sections used in this work the isotopic ratio at production (shown in Fig. 2) has a value of order 0.6–0.8, with only a weak energy dependence. Assuming the validity of these cross section models implies that: (i) the effects of decay are significant and suppress the spectrum of the unstable isotope Be10, and (ii) the effects of decay have a weak energy dependence, even when the decay time changes by a large factor.

The predictions of the two models for the nuclear fragmentation cross sections have some significant differences. Using the Evoli et al. cross section model [8] the isotopic ratio at production grows from a value $R_0 \simeq 0.59$ at for $E_0 \simeq 1$ GeV to an asymptotic value $R_0 \simeq 0.81$ at asymptotic value of order 0.80 at high energy. Using the GALPROP model [11] the prediction for the isotopic ratio at production is $R_0 \simeq 0.64$ at $E_0 \simeq 1$ GeV and decreases to an asymptotic value of order 0.60 at high energy, therefore in this case one obtains an average survival probability that is a little larger and that grows a little more rapidly with energy. However, for both models, the growth of P_{surv} is only slow, and interpreting the results in the framework of the Minimal Diffusion Model one obtains a diffusion time that increases with energy (see Fig. 3).

An average cosmic ray age that increases with energy is not only in conflict with the standard interpretation of the secondary/primary ratio that estimate a grammage that decreases with rigidity, but is also very difficult to understand constructing a model for the magnetic structure of the Galaxy. The alternative is to modify the theoretical framework for the interpretation of the results on $P_{\text{surv}}(E_0)$. In this

work have shown (see for example Fig. 6) that the same value of P_{surv} can correspond to very different values of the average age of the CR particles in different propagation models. Similarly, a measurement of the energy dependence of the survival probability $P_{\text{surv}}(E_0)$ can be interpreted with different energy dependences of the propagation parameters in different propagation models.

It is easy to see that a survival probability that changes very slowly with energy can be consistent with an average age that is constant or change very slowly with energy if the shape of the age distribution is very broad.

If the CR age distribution is broad, the average survival probability P_{surv} takes (in first approximation) the physical meaning of the fraction of the observed particles with age in the interval $t_{\text{age}} \lesssim T_{\text{dec}}(E_0)$. The decay time grows linearly with the Lorentz factor of the nuclei, and therefore, for a constant shape of the age distribution, P_{surv} increases with energy because the time interval where decay is important becomes smaller. This growth of P_{surv} with energy is slower for a broader distribution.

In the Minimal Diffusion Model the age distribution is determined by two parameters the diffusion times and the halo vertical size. It is however possible for the age distribution to have a more complicated shape that depends on more parameters (that could have different energy dependences). The preliminary AMS02 data (interpreted with current models of the fragmentation cross sections) indicate that when the decay time grows from approximately 4 Myr to approximately 30 Myr the average survival probability remains in rather narrow range ($P_{\text{surv}} \simeq 0.25\text{--}0.4$) suggesting a very broad age distribution where large fractions of particles have ages that are both very short ($t_{\text{age}} \lesssim \text{few Myr}$) and very long ($t_{\text{age}} \gtrsim 50 \text{ few Myr}$). This broad age distribution could exist if the CR confinement volume is formed by an inner halo and a more extended halo (perhaps associated with the existence of the Fermi bubbles) that have confinement times of different orders of magnitude.

The estimate of the CR age distribution is crucially important for the interpretation of the electron and positron spectra, in particular to establish the existence of a new source of relativistic positrons [34–36]. A sufficiently long CR age implies that the large rate of energy losses for e^\pm spectra will result in a strong softening of their spectra, and therefore that the observed hard positron spectrum cannot be generated by the secondary production mechanism and requires a harder source. The preliminary AMS02 beryllium data, as interpreted in the previous section, indicate a CR age that seems to be in conflict with the hypothesis of secondary production for CR positrons. This conclusion is again based on the validity of the current estimates of the nuclear fragmentation cross sections. An approximately constant isotopic ratio for beryllium could in principle be consistent with energy independent fragmentation cross sections and with a short CR age, so that the decay effects for Be10 are small in the entire energy range considered. This interpretation however requires that the observed isotopic composition is equal to the one generated at injection, and this hypothesis is at present strongly disfavoured.

The modeling of nuclear fragmentation cross sections is the main source of systematic uncertainties in extracting the very valuable information encoded in the beryllium isotopic composition. Reducing these uncertainties with an appropriate program of experimental studies is very desirable and of great value.

Acknowledgments

I'm grateful to Pedro De la Torre Luque for help in obtaining the GALPROP nuclear fragmentation cross sections, and to Carmelo Evoli and Michael Korsmeier for interesting discussions.

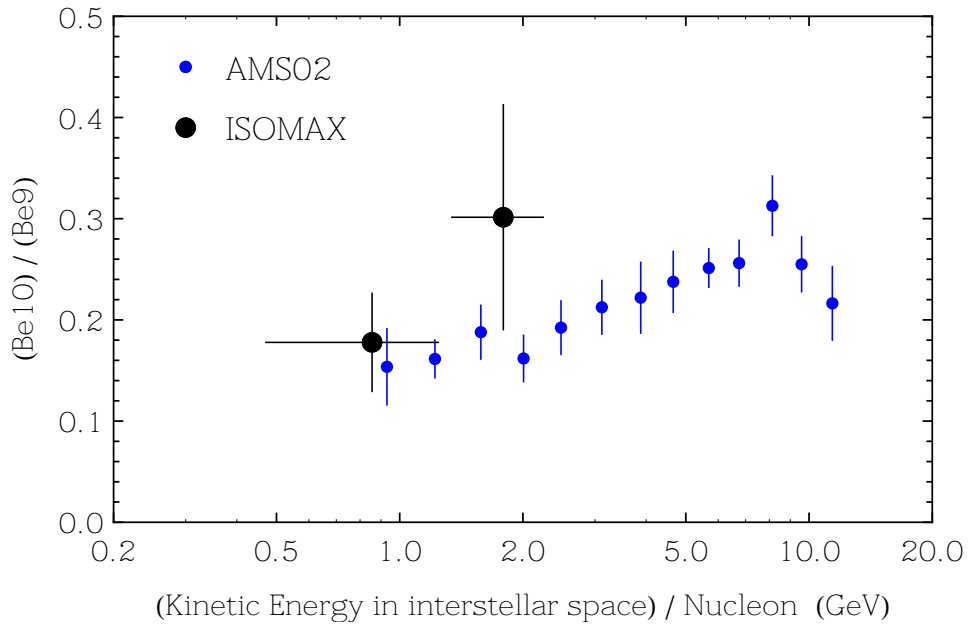


FIG. 1: Measurements of the isotopic ratio beryllium-10/beryllium-9 at high energy, plotted as a function of kinetic energy per nucleon. The data is from ISOMAX [3] and (only preliminary) from AMS02 [2].

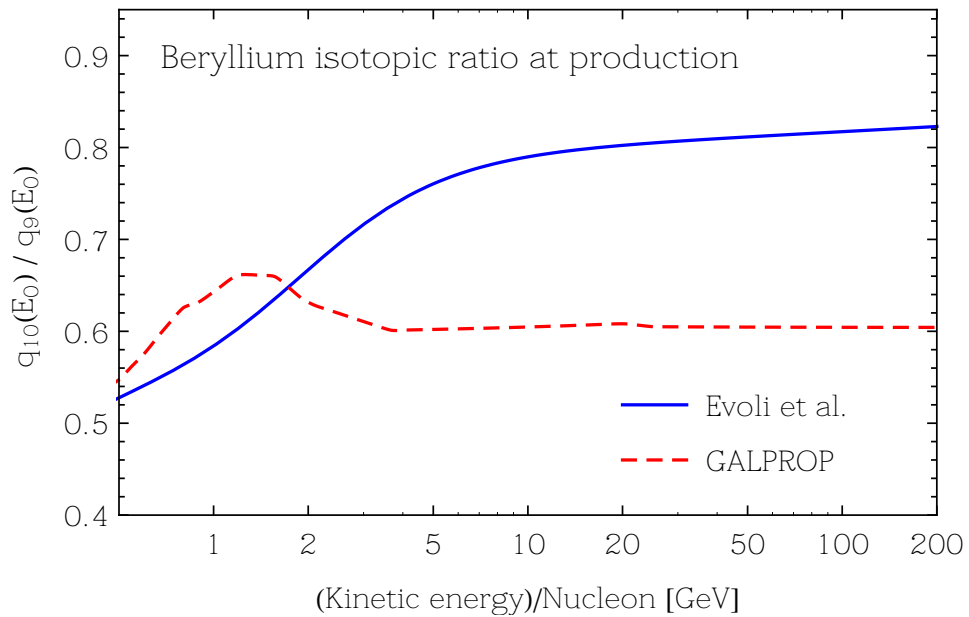


FIG. 2: Ratio of the production rates of beryllium-10 and beryllium-9 plotted as a function of kinetic energy per nucleon. The ratio is calculated assuming for the interacting cosmic ray particles the energy spectra measured by AMS02 [7], and for the nuclear fragmentation cross sections the values tabulated in Evoli et al. [8] and those in the GALPROP code [11]. The calculation includes only the leading contribution of interactions with an hydrogen target.

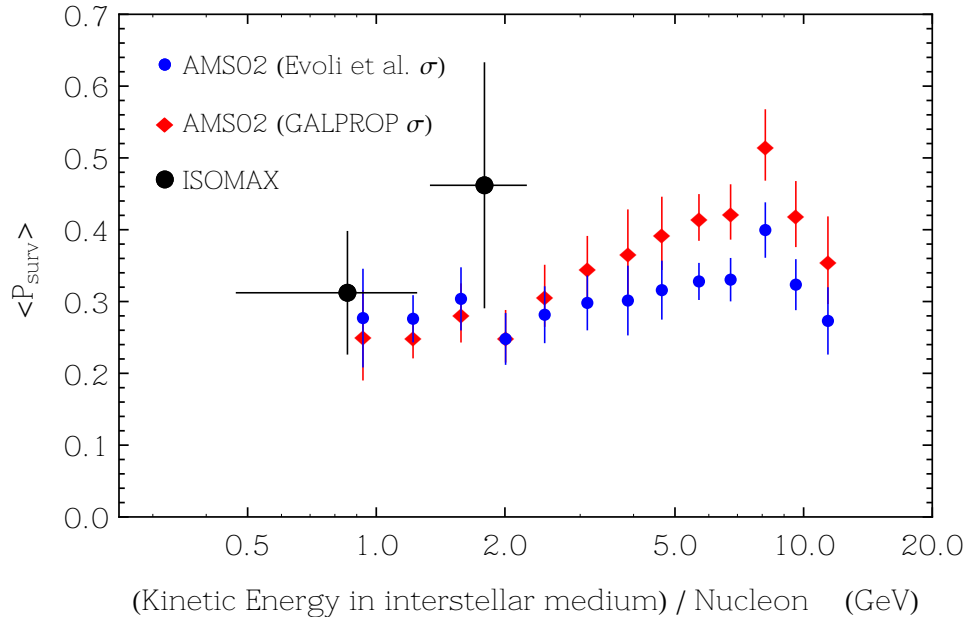


FIG. 3: Estimate of the average survival probability $P_{\text{surv}}(E_0)$ of beryllium-10 nuclei, as a function of kinetic energy per nucleon in the local interstellar medium. The probability is estimated from the measurements of the beryllium isotopic ratio $\text{Be}190/\text{Be}9$ by ISOMAX [3] and AMS02 [2], including corrections for solar modulations, and assuming constant energy during propagation in interstellar space. The isotopic ratio at injection is calculated using the nuclear fragmentation cross sections of Evoli et. al. [8] and of GALPROP [11].

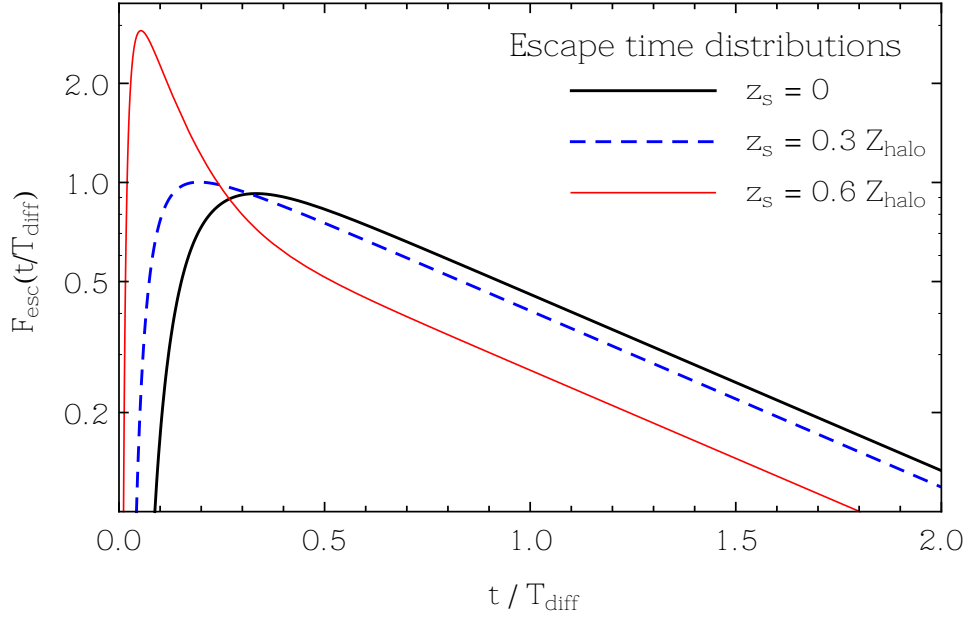


FIG. 4: Escape time distribution for the simple diffusion model, shown as a function of the ratio t/T_{diff} . The three curves correspond to three different injection points ($z_s/Z_{\text{halo}} = 0, 0.3$ and 0.6). The distribution at large t becomes asymptotically an exponential with slope $T^* = (8/\pi^2) T_{\text{diff}}$.

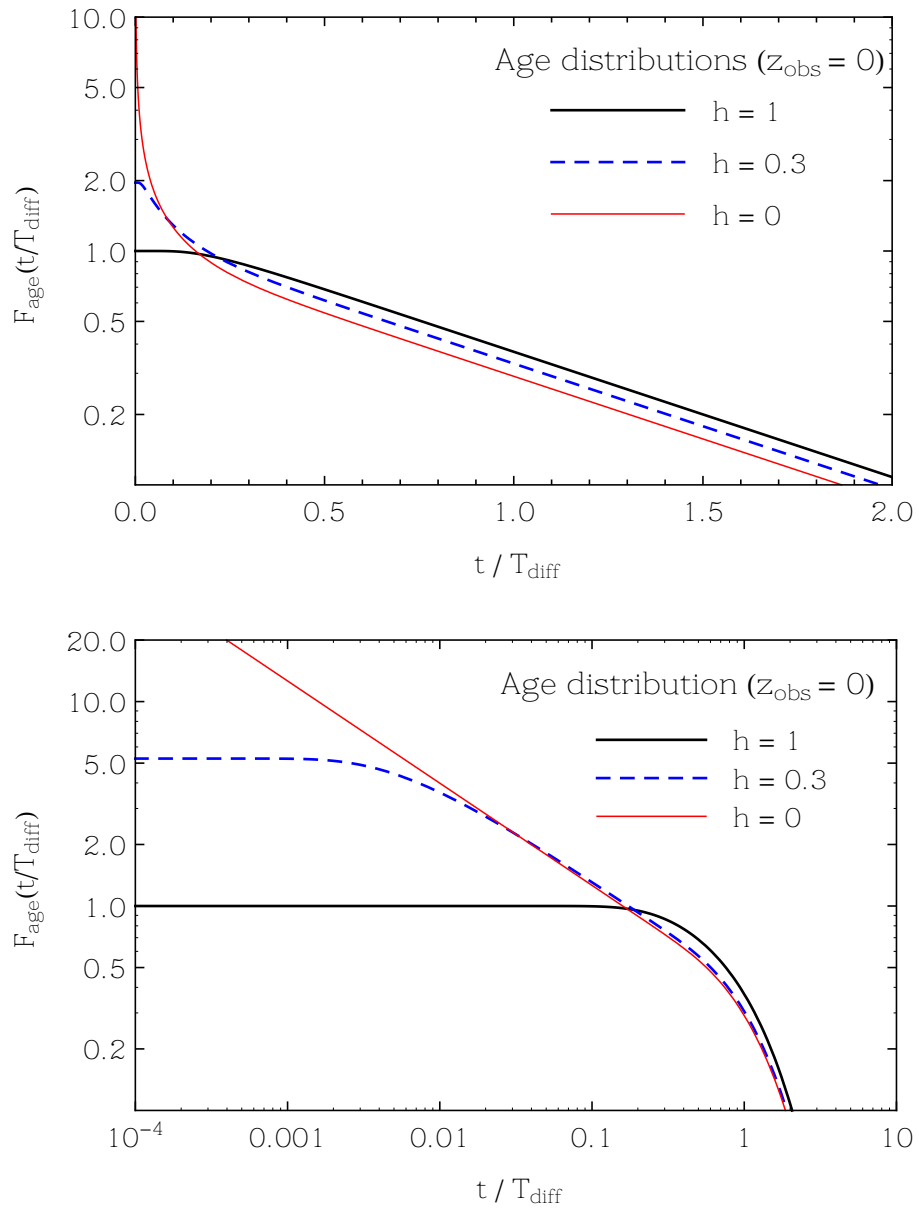


FIG. 5: Top panel: age distribution in the simple diffusion model, shown as a function of t/T_{diff} . The curves are calculated for an observation point on the Galactic plane ($z_{\text{obs}} = 0$) and for three choices of the ratio $Z_{\text{disk}}/Z_{\text{halo}}$ (1, 0.3 and 0). Bottom panel: the same curves are shown plotted with a log-log scale .

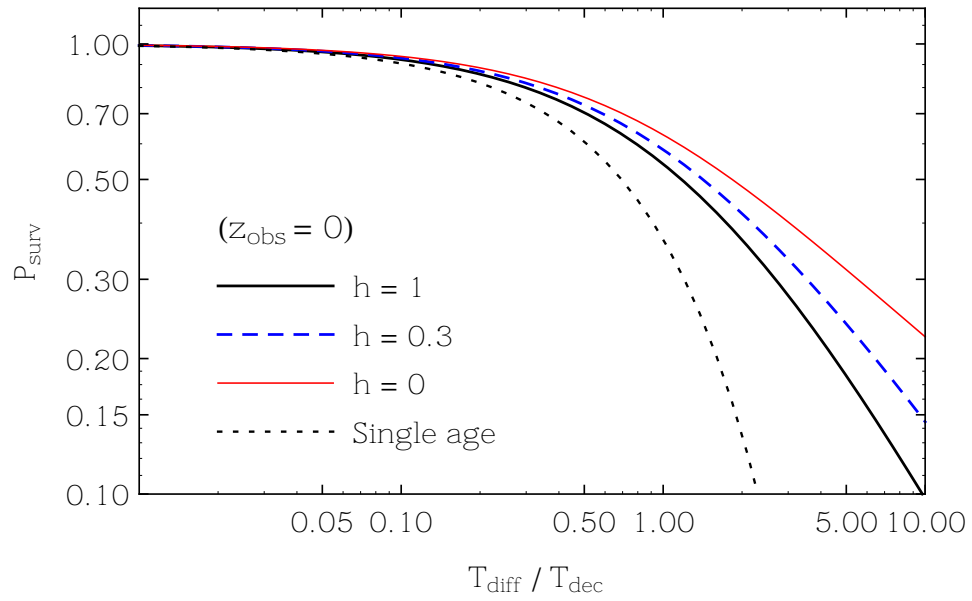


FIG. 6: Average survival probability calculated for the Minimal Diffusion Model, for an observation point on the Galactic plane ($z_{\text{obs}} = 0$), and plotted as a function of the ratio $T_{\text{diff}}/T_{\text{dec}}$. The different curves are calculated for three values of the ratio $h = Z_{\text{disk}}/Z_{\text{halo}}$ ($h = 0, 0.3$ and 1). The dotted line corresponds to a narrow age distribution.

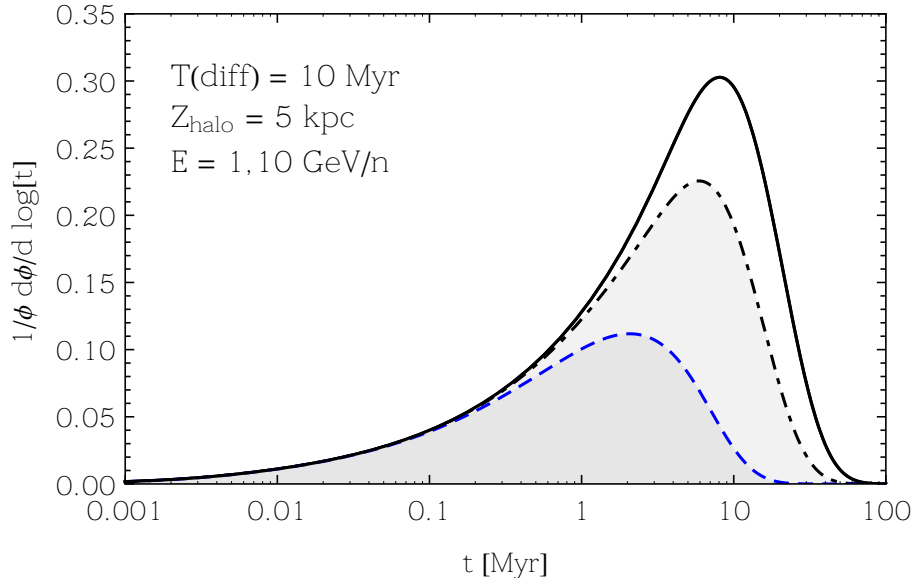


FIG. 7: The solid line shows an example of the age distribution calculated in the simple diffusion model (for the choice of parameters $T_{\text{diff}} = 10 \text{ Myr}$, $Z_{\text{halo}} = 5 \text{ kpc}$, $s = 0$). The dashed (dot-dashed) line is the distribution calculated including the effects of decay for Be10 nuclei with kinetic energy per nucleon $E_0 = 1$ (10) GeV. The average survival probability is the ratio between the areas calculated including and neglecting the effects of decay.

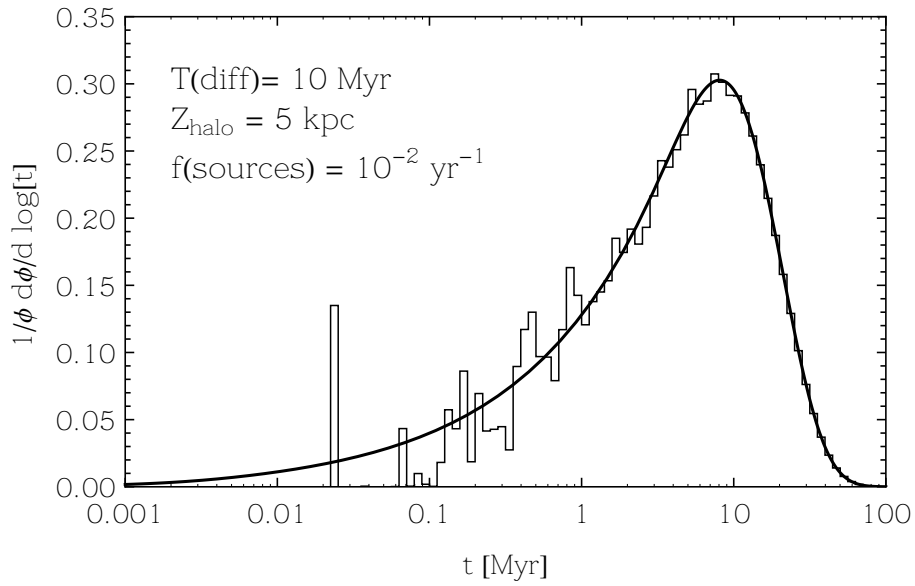


FIG. 8: The solid line shows an example of the age distribution calculated in the simple diffusion model (for the choice of parameters $T_{\text{diff}} = 10 \text{ Myr}$, $Z_{\text{halo}} = 5 \text{ kpc}$, $s = 0$), calculated assuming that the injection of CR particles is continuous in space and time. The histogram is one Monte Carlo realisation of the age distribution calculated assuming that the injection has (after averaging) the same distribution, but is formed by an ensemble of discrete, instantaneous and point-like events.

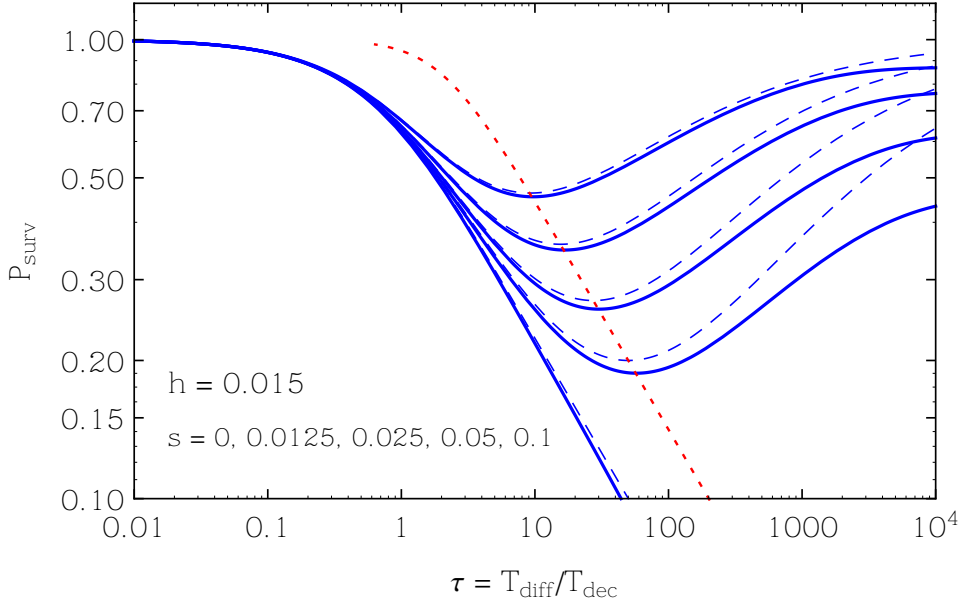


FIG. 9: Solid lines: average survival probability $P_{\text{surv}}(\tau, s, h)$ plotted as function of τ for one value of the ratio $h = Z_{\text{disk}}/Z_{\text{halo}} = 0.015$ and different values of s ($s = 0, 0.0125, 0.025, 0.05$ and 0.1). The dashed lines show the average survival probability for the same values of s , but for $h = 0$. The dotted (red) line is the parametric curve $\{\tau^*(s), P_{\text{surv}}^*(s)\}$ [see Eqs. (48) and (49)] and describes the positions of the minima of the survival probability for small h .

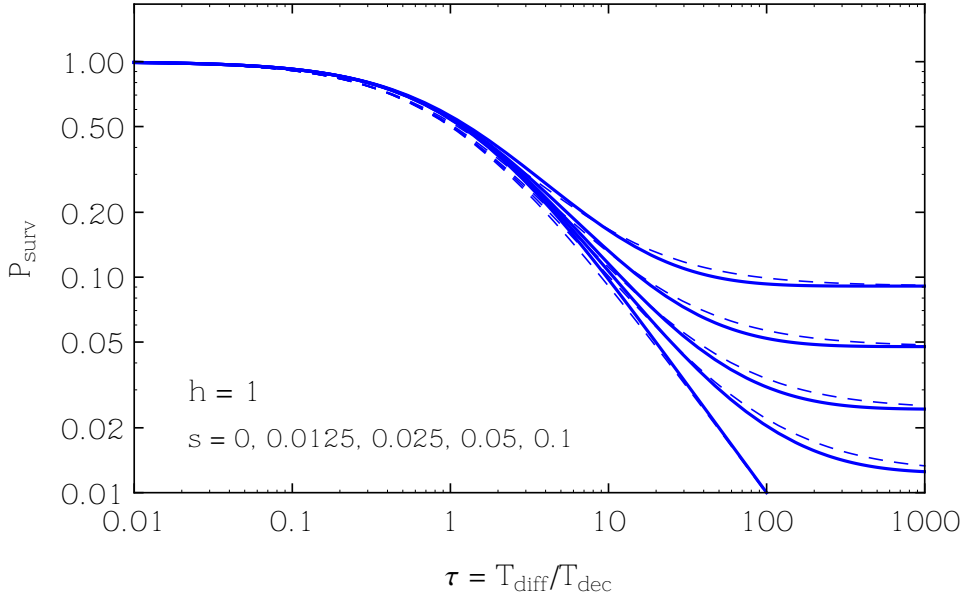


FIG. 10: Solid lines: average survival probability $P_{\text{surv}}(\tau, s, h)$ plotted as function of τ for a constant value $h = 1$ and different values of s ($s = 0, 0.0125, 0.025, 0.05$ and 0.1). The dashed lines show the survival probability in the leaky box model.

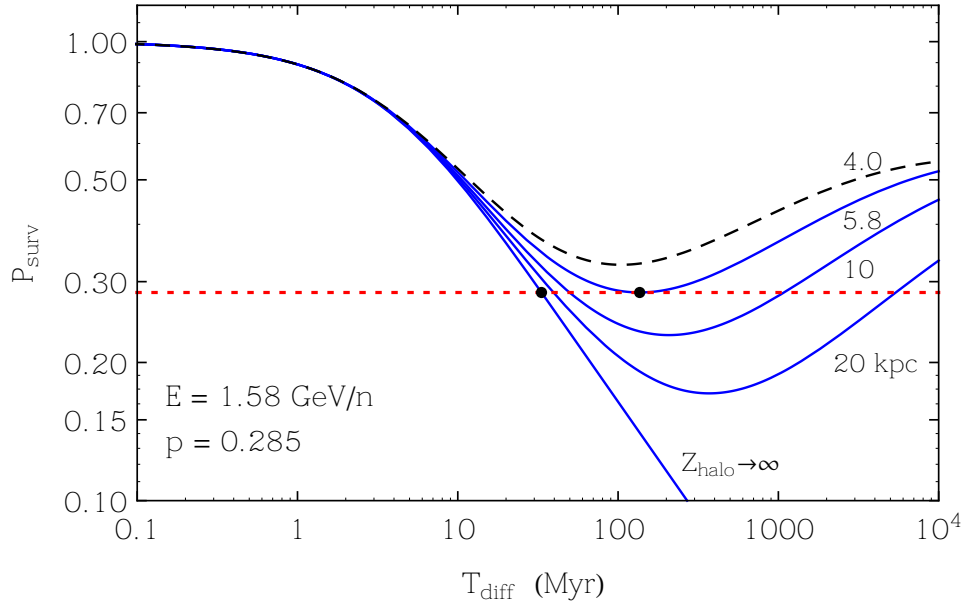


FIG. 11: The solid lines show the average survival probability plotted as a function of the diffusion time T_{diff} for beryllium nuclei of energy $E_0 = 1.57$ GeV/n (when $T_{\text{dec}} \simeq 5.4$ Myr) for different values of the vertical halo size Z_{halo} . A fixed value of the average survival probability corresponds to allowed ranges of T_{diff} and Z_{halo} . The figure illustrates the case for $P_{\text{surv}} \simeq 0.285$ (the central value inferred from the AMS02 measurement using the GALPROP nuclear fragmentation cross sections). The minimum allowed T_{diff} corresponds to $Z_{\text{halo}} \rightarrow \infty$, while the maximum value corresponds to the smallest halo size, and also to the situation where the observed P_{surv} is the a minimum (for a fixed value of Z_{halo}).

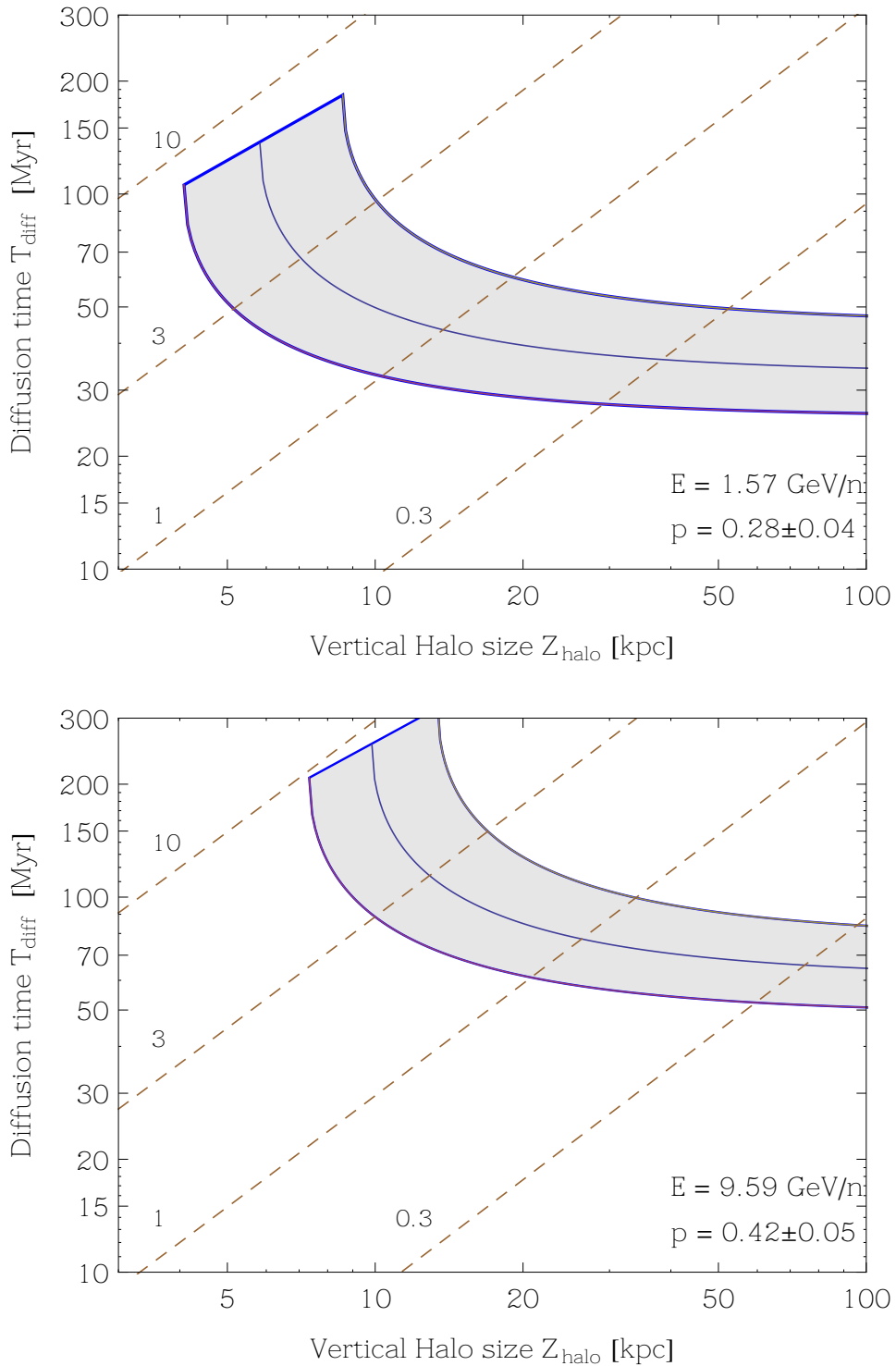


FIG. 12: Allowed regions in the space $\{Z_{\text{halo}}, T_{\text{diff}}\}$ for a measurement of the average survival probability in the simple diffusion model. The top (bottom) panel is for the AMS02 measurement at $E_0 = 1.57$ and 9.59 GeV , estimating the average survival probability with the GALPROP cross sections.

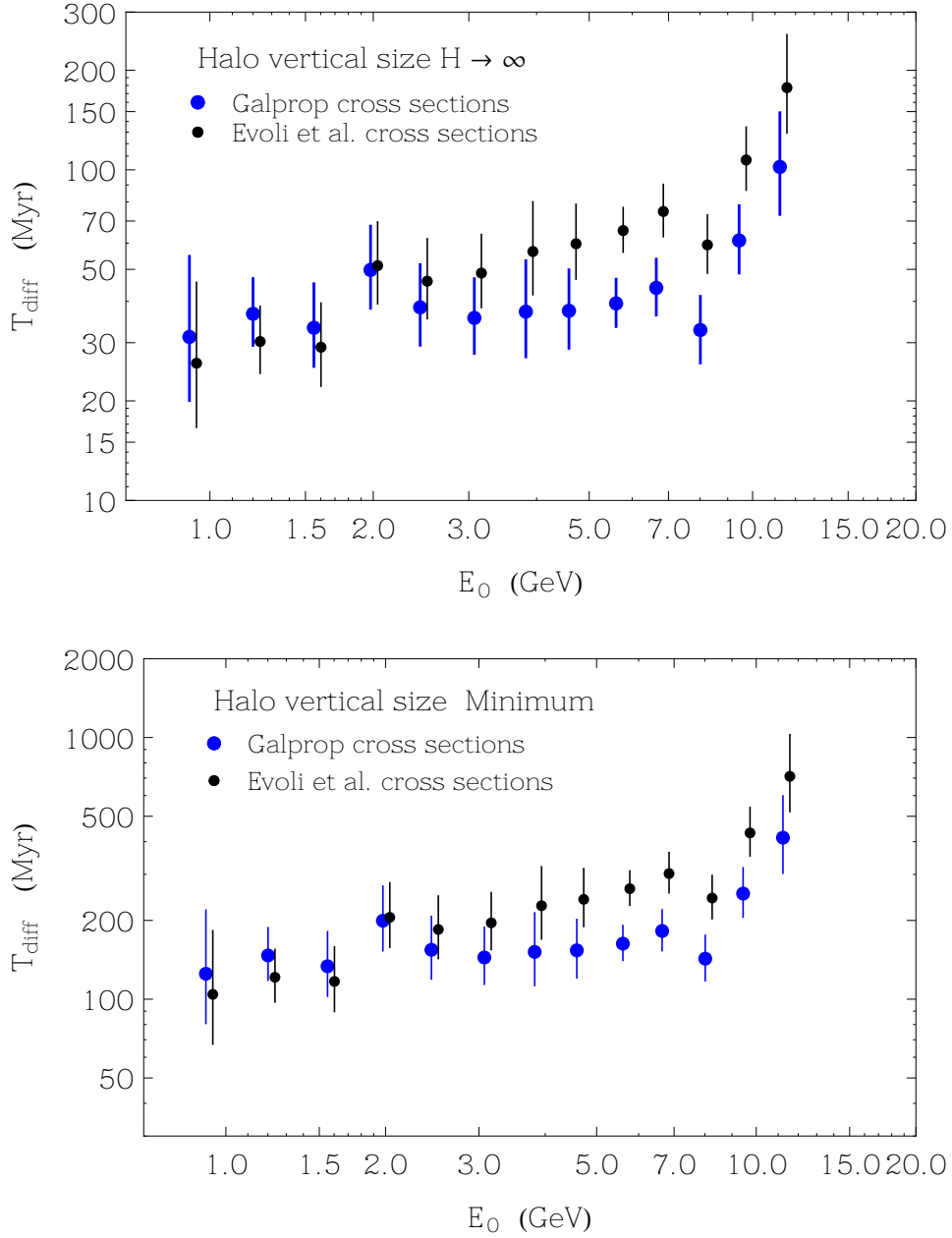


FIG. 13: Estimates of the diffusion times obtained from the AMS02 measurements of the beryllium isotopic ratio in the simple diffusion model. The survival probability is calculated using the Evoli et al. [8], or the GALPROP [11] cross sections. In the top panel the diffusion time is calculated neglecting the effect of interactions (that is in the limit $Z_{\text{halo}} \rightarrow \infty$). In the bottom panel the halo size has the minimum allowed value.

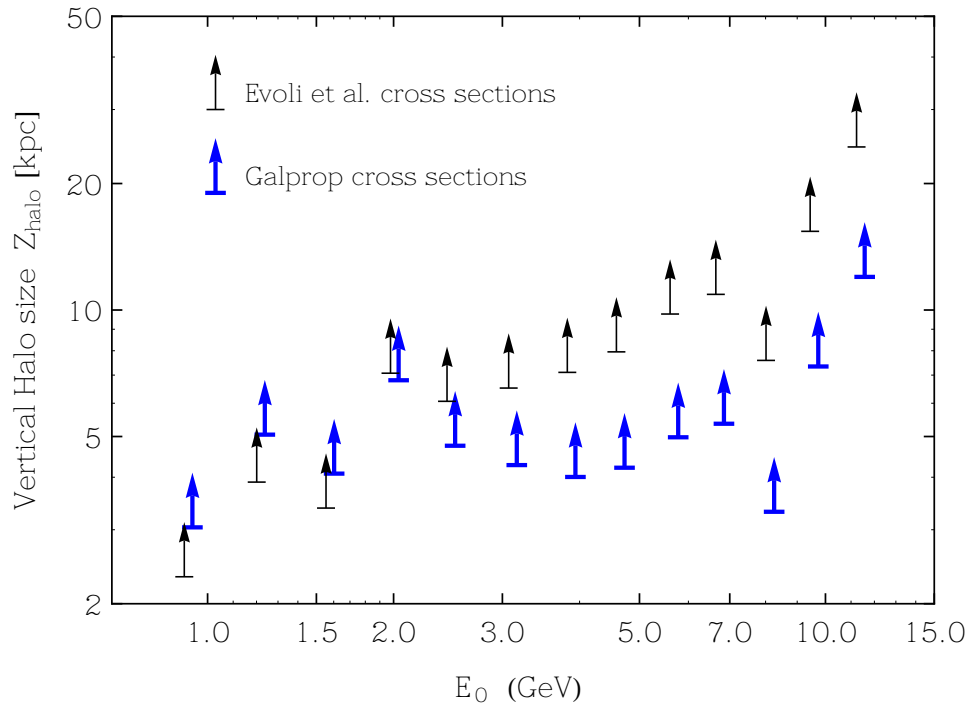


FIG. 14: Lower limit on the CR vertical halo size obtained from the AMS02 measurement of the beryllium isotopic ratio calculated in the framework of the simple diffusion model. The two estimates are obtained using the nuclear fragmentation cross sections of Evoli et al. [8], and of GALPROP [11].

-
- [1] P. Lipari, “The lifetime of cosmic rays in the Milky Way,” [arXiv:1407.5223 [astro-ph.HE]].
- [2] L. Derome for the AMS02 Collaboration, “Cosmic-Ray Lithium & Beryllium Isotopes with AMS02” Contribution at the 37th International Cosmic Ray Conference. Available at <https://indico.desy.de/event/27991/contributions/101805/>.
- [3] T. Hams, *et al.*, “Measurement of the abundance of radioactive Be-10 and other light isotopes in cosmic radiation up to 2-GeV/nucleon with the balloon-borne instrument ISOMAX,” *Astrophys. J.* **611**, 892-905 (2004) doi:10.1086/422384
- [4] S. P. Ahlen *et al.*, “Measurement of the Isotopic Composition of Cosmic-Ray Helium, Lithium, Beryllium, and Boron up to 1700 MEV per Atomic Mass Unit” *Astrop.J.* **534**, 757 (2000). DOI: 10.1086/308762
- [5] J. J. Connell, “Galactic Cosmic-Ray Confinement Time: Ulysses High Energy Telescope Measurements of the Secondary Radionuclide ^{10}Be ” *Ap.J.* **501**, L59, (1998). DOI: 10.1086/311437
- [6] N. E. Yanasak *et al.*, “Measurement of the Secondary Radionuclides ^{10}Be , ^{26}Al , ^{36}Cl , ^{54}Mn , and ^{14}C and Implications for the Galactic Cosmic-Ray Age”, *Astrop. J.* **563**, 768 (2001). DOI: 10.1086/323842
- [7] M. Aguilar *et al.* [AMS], “The Alpha Magnetic Spectrometer (AMS) on the international space station: Part II — Results from the first seven years,” *Phys. Rept.* **894**, 1-116 (2021) doi:10.1016/j.physrep.2020.09.003
- [8] C. Evoli, R. Aloisio and P. Blasi, “Galactic cosmic rays after the AMS-02 observations,” *Phys. Rev. D* **99**, no.10, 103023 (2019) doi:10.1103/PhysRevD.99.103023 [arXiv:1904.10220 [astro-ph.HE]].
- [9] I. V. Moskalenko and A. W. Strong, “Production and propagation of cosmic ray positrons and electrons,” *Astrophys. J.* **493**, 694-707 (1998) doi:10.1086/305152 [arXiv:astro-ph/9710124 [astro-ph]].
- [10] A. W. Strong and I. V. Moskalenko, “Propagation of cosmic-ray nucleons in the galaxy,” *Astrophys. J.* **509**, 212-228 (1998) doi:10.1086/306470 [arXiv:astro-ph/9807150 [astro-ph]].
- [11] I. Moskalenko, G. Jóhannesson and T. Porter, “GALPROP Code for Galactic Cosmic Ray Propagation and Associated Photon Emissions,” *PoS ICRC2021*, 152 (2021) doi:10.22323/1.395.0152
- [12] Giuseppe Cocconi, “On the Origin of the Cosmic Radiation”, *Phys. Rev.* **83**, 1193 (1951). DOI: 10.1103/PhysRev.83.1193
- [13] E. Fermi, “On the Origin of the Cosmic Radiation,” *Phys. Rev.* **75**, 1169-1174 (1949) doi:10.1103/PhysRev.75.1169
- [14] P. Morrison, S. Olbert. B. Rossi, “The Origin of Cosmic Rays”, *Phys. Rev.* **94**, 440 (1954). doi:10.1103/PhysRev.94.440
- [15] V. L. Ginzburg and S. I. Syrovatskii, “The Origin of Cosmic Rays”, Pergamon Press (1964).
- [16] C. Evoli, *et al.*, “Cosmic-ray propagation with DRAGON2: I. numerical solver and astrophysical ingredients,” *JCAP* **02**, 015 (2017) doi:10.1088/1475-7516/2017/02/015 [arXiv:1607.07886 [astro-ph.HE]].
- [17] C. Evoli, D. Gaggero, A. Vittino, M. Di Mauro, D. Grasso and M. N. Mazziotta, “Cosmic-ray propagation with DRAGON2: II. Nuclear interactions with the interstellar gas,” *JCAP* **07**, 006 (2018) doi:10.1088/1475-7516/2018/07/006 [arXiv:1711.09616 [astro-ph.HE]].
- [18] M. Boudaud and D. A. Maurin, “Galactic cosmic nuclei and leptons with USINE,” *PoS ICRC2017*, 255 (2018) doi:10.22323/1.301.0255
- [19] R. Kissmann, “Galactic cosmic ray propagation models using Picard,” *J. Phys. Conf. Ser.* **837**, no.1, 012003 (2017) doi:10.1088/1742-6596/837/1/012003
- [20] K. M. Ferriere, “The interstellar environment of our galaxy,” *Rev. Mod. Phys.* **73**, 1031-1066 (2001) doi:10.1103/RevModPhys.73.1031 [arXiv:astro-ph/0106359 [astro-ph]].
- [21] J. J. Engelmann, P. Ferrando, A. Soutoul, P. Goret and E. Juliusson, “Charge composition and energy spectra of cosmic-ray for elements from Be to Ni - Results from HEAO-3-C2,” *Astron. Astrophys.* **233**, 96-111 (1990)
- [22] C. Evoli, G. Morlino, P. Blasi and R. Aloisio, “AMS-02 beryllium data and its implication for cosmic ray transport,” *Phys. Rev. D* **101**, no.2, 023013 (2020) doi:10.1103/PhysRevD.101.023013 [arXiv:1910.04113 [astro-ph.HE]].
- [23] M. J. Boschini, *et al.*, “Deciphering the local Interstellar spectra of primary cosmic ray species with HelMod”, *Astrophys. J.* **858**, no.1, 61 (2018) doi:10.3847/1538-4357/aabc54 [arXiv:1804.06956 [astro-ph.HE]].
- [24] M. J. Boschini, *et al.*, “Deciphering the local Interstellar spectra of secondary nuclei with GALPROP/HelMod framework and a hint for primary lithium in cosmic rays,” *Astrophys. J.* **889**, 167 (2020) doi:10.3847/1538-4357/ab64f1 [arXiv:1911.03108 [astro-ph.HE]].
- [25] N. Weinrich, *et al.*, “Combined analysis of AMS-02 (Li,Be,B)/C, N/O, ^3He , and ^4He data,” *Astron. Astrophys.* **639**, A131 (2020) doi:10.1051/0004-6361/202037875 [arXiv:2002.11406 [astro-ph.HE]].
- [26] N. Weinrich, *et al.*, “Galactic halo size in the light of recent AMS-02 data,” *Astron. Astrophys.* **639**, A74 (2020) doi:10.1051/0004-6361/202038064 [arXiv:2004.00441 [astro-ph.HE]].
- [27] Y. Génolini, *et al.*, “New minimal, median, and maximal propagation models for dark matter searches

- with Galactic cosmic rays,” *Phys. Rev. D* **104**, no.8, 083005 (2021) doi:10.1103/PhysRevD.104.083005 [arXiv:2103.04108 [astro-ph.HE]].
- [28] P. D. Luque, M. N. Mazziotta, F. Loparco, F. Gargano and D. Serini, “Markov chain Monte Carlo analyses of the flux ratios of B, Be and Li with the DRAGON2 code,” *JCAP* **07**, 010 (2021) doi:10.1088/1475-7516/2021/07/010 [arXiv:2102.13238 [astro-ph.HE]].
- [29] M. Korsmeier and A. Cuoco, “Implications of Lithium to Oxygen AMS-02 spectra on our understanding of cosmic-ray diffusion,” *Phys. Rev. D* **103**, no.10, 103016 (2021) doi:10.1103/PhysRevD.103.103016 [arXiv:2103.09824 [astro-ph.HE]].
- [30] R. Cowsik and L.W. Wilson, “The Nested Leaky-Box Model for Galactic Cosmic Rays” In Proc. 14th ICRC, vol. 2, p.659 (1975).
- [31] R. Cowsik, B. Burch and T. Madziwa-Nussinov, “The origin of the spectral intensities of cosmic-ray positrons,” *Astrophys. J.* **786**, 124 (2014) doi:10.1088/0004-637X/786/2/124 [arXiv:1305.1242 [astro-ph.HE]].
- [32] R. Cowsik and T. Madziwa-Nussinov, “Spectral Intensities of Antiprotons and the Nested Leaky-box Model for Cosmic Rays in the Galaxy,” *Astrophys. J.* **827**, no.2, 119 (2016) doi:10.3847/0004-637X/827/2/119
- [33] R. Cowsik, “Positrons and Antiprotons in Galactic Cosmic Rays,” *Ann. Rev. Nucl. Part. Sci.* **66**, 297-319 (2016) doi:10.1146/annurev-nucl-102115-044851
- [34] P. Lipari, “Interpretation of the cosmic ray positron and antiproton fluxes,” *Phys. Rev. D* **95**, no.6, 063009 (2017) doi:10.1103/PhysRevD.95.063009 [arXiv:1608.02018 [astro-ph.HE]].
- [35] P. Lipari, “Spectral shapes of the fluxes of electrons and positrons and the average residence time of cosmic rays in the Galaxy,” *Phys. Rev. D* **99**, no.4, 043005 (2019) doi:10.1103/PhysRevD.99.043005 [arXiv:1810.03195 [astro-ph.HE]].
- [36] P. Lipari, “Understanding the cosmic ray positron flux,” [arXiv:1902.06173 [astro-ph.HE]].